



# TECH BRIEFS

NATIONAL AERONAUTICS AND SPACE ADMINISTRATION

-  **Technology Focus**
-  **Computers/Electronics**
-  **Software**
-  **Materials**
-  **Mechanics**
-  **Machinery/Automation**
-  **Manufacturing**
-  **Bio-Medical**
-  **Physical Sciences**
-  **Information Sciences**
-  **Books and Reports**



## INTRODUCTION

Tech Briefs are short announcements of innovations originating from research and development activities of the National Aeronautics and Space Administration. They emphasize information considered likely to be transferable across industrial, regional, or disciplinary lines and are issued to encourage commercial application.

### Availability of NASA Tech Briefs and TSPs

Requests for individual Tech Briefs or for Technical Support Packages (TSPs) announced herein should be addressed to

#### National Technology Transfer Center

Telephone No. (800) 678-6882 or via World Wide Web at [www2.nttc.edu/leads/](http://www2.nttc.edu/leads/)

Please reference the control numbers appearing at the end of each Tech Brief. Information on NASA's Commercial Technology Team, its documents, and services is also available at the same facility or on the World Wide Web at [www.nctn.hq.nasa.gov](http://www.nctn.hq.nasa.gov).

Innovative Partnerships Offices are located at NASA field centers to provide technology-transfer access to industrial users. Inquiries can be made by contacting NASA field centers and Mission Directorates listed below.

## NASA Field Centers and Program Offices

#### Ames Research Center

Lisa L. Lockyer  
(650) 604-1754  
[lisa.l.lockyer@nasa.gov](mailto:lisa.l.lockyer@nasa.gov)

#### Dryden Flight Research Center

Gregory Poteat  
(661) 276-3872  
[greg.poteat@dfrc.nasa.gov](mailto:greg.poteat@dfrc.nasa.gov)

#### Goddard Space Flight Center

Nona Cheeks  
(301) 286-5810  
[Nona.K.Cheeks.1@nasa.gov](mailto:Nona.K.Cheeks.1@nasa.gov)

#### Jet Propulsion Laboratory

Ken Wolfenbarger  
(818) 354-3821  
[james.k.wolfenbarger@jpl.nasa.gov](mailto:james.k.wolfenbarger@jpl.nasa.gov)

#### Johnson Space Center

Helen Lane  
(713) 483-7165  
[helen.w.lane@nasa.gov](mailto:helen.w.lane@nasa.gov)

#### Kennedy Space Center

Jim Aliberti  
(321) 867-6224  
[Jim.Aliberti-1@nasa.gov](mailto:Jim.Aliberti-1@nasa.gov)

#### Langley Research Center

Ray P. Turcotte  
(757) 864-8881  
[r.p.turcotte@larc.nasa.gov](mailto:r.p.turcotte@larc.nasa.gov)

#### John H. Glenn Research Center at Lewis Field

Robert Lawrence  
(216) 433-2921  
[robert.f.lawrence@nasa.gov](mailto:robert.f.lawrence@nasa.gov)

#### Marshall Space Flight Center

Vernotto McMillan  
(256) 544-2615  
[vernotto.mcmillan@msfc.nasa.gov](mailto:vernotto.mcmillan@msfc.nasa.gov)

#### Stennis Space Center

John Bailey  
(228) 688-1660  
[john.w.bailey@nasa.gov](mailto:john.w.bailey@nasa.gov)

#### NASA Mission Directorates

At NASA Headquarters there are four Mission Directorates under which there are seven major program offices that develop and oversee technology projects of potential interest to industry:

##### Carl Ray

Small Business Innovation Research Program (SBIR) & Small Business Technology Transfer Program (STTR)  
(202) 358-4652  
[carl.g.ray@nasa.gov](mailto:carl.g.ray@nasa.gov)

##### Frank Schowengerdt

Innovative Partnerships Program (Code TD)  
(202) 358-2560  
[fschowen@hq.nasa.gov](mailto:fschowen@hq.nasa.gov)

##### John Mankins

Exploration Systems Research and Technology Division  
(202) 358-4659  
[john.c.mankins@nasa.gov](mailto:john.c.mankins@nasa.gov)

##### Terry Hertz

Aeronautics and Space Mission Directorate  
(202) 358-4636  
[thertz@mail.hq.nasa.gov](mailto:thertz@mail.hq.nasa.gov)

##### Glen Mucklow

Mission and Systems Management Division (SMD)  
(202) 358-2235  
[gmucklow@mail.hq.nasa.gov](mailto:gmucklow@mail.hq.nasa.gov)

##### Granville Paules

Mission and Systems Management Division (SMD)  
(202) 358-0706  
[gpaules@mtpe.hq.nasa.gov](mailto:gpaules@mtpe.hq.nasa.gov)

##### Gene Trinh

Human Systems Research and Technology Division (ESMD)  
(202) 358-1490  
[eugene.h.trinh@nasa.gov](mailto:eugene.h.trinh@nasa.gov)

##### John Rush

Space Communications Office (SOMD)  
(202) 358-4819  
[john.j.rush@nasa.gov](mailto:john.j.rush@nasa.gov)





# TECH BRIEFS

NATIONAL AERONAUTICS AND SPACE ADMINISTRATION



## 5 Technology Focus: Test & Measurement

- 5 Apparatus Characterizes Transient Voltages in Real Time
- 6 Measuring Humidity in Sealed Glass Encasements
- 7 Adaptable System for Vehicle Health and Usage Monitoring
- 8 Miniature Focusing Time-of-Flight Mass Spectrometer
- 9 Cryogenic High-Sensitivity Magnetometer
- 10 Wheel Electrometer System



## 11 Electronics/Computers

- 11 Carbon-Nanotube Conductive Layers for Thin-Film Solar Cells
- 12 Patch Antenna Fed via Unequal-Crossed-Arm Aperture
- 12 LC Circuits for Diagnosing Embedded Piezoelectric Devices
- 13 Nanowire Thermoelectric Devices



## 15 Software

- 15 Code for Analyzing and Designing Spacecraft Power System Radiators
- 15 Decision Support for Emergency Operations Centers
- 15 NASA Records Database
- 16 Real-Time Principal-Component Analysis
- 16 Fuzzy/Neural Software Estimates Costs of Rocket-Engine Tests



## 17 Materials

- 17 Multicomponent, Rare-Earth-Doped Thermal-Barrier Coatings
- 17 Reactive Additives for Phenylethynyl-Containing Resins



## 19 Mechanics

- 19 Improved Gear Shapes for Face Worm Gear Drives

- 20 Alternative Way of Shifting Mass To Move a Spherical Robot



## 21 Manufacturing

- 21 Parylene C as a Sacrificial Material for Microfabrication
- 21 *In Situ* Electrochemical Deposition of Microscopic Wires
- 22 Improved Method of Manufacturing SiC Devices



## 25 Bio-Medical

- 25 Microwave Treatment of Prostate Cancer and Hyperplasia



## 27 Physical Sciences

- 27 Ferroelectric Devices Emit Charged Particles and Radiation
- 28 Dusty-Plasma Particle Accelerator
- 29 Frozen-Plug Technique for Liquid-Oxygen Plumbing



## 31 Books & Reports

- 31 Shock Waves in a Bose-Einstein Condensate
- 31 Progress on a Multichannel, Dual-Mixer Stability Analyzer
- 31 Development of Carbon-Nanotube/Polymer Composites
- 31 Thermal Imaging of Earth for Accurate Pointing of Deep-Space Antennas
- 31 Modifications of a Composite-Material Combustion Chamber
- 32 Modeling and Diagnostic Software for Liquefying-Fuel Rockets
- 32 Spacecraft Antenna Clusters for High EIRP

This document was prepared under the sponsorship of the National Aeronautics and Space Administration. Neither the United States Government nor any person acting on behalf of the United States Government assumes any liability resulting from the use of the information contained in this document, or warrants that such use will be free from privately owned rights.





## Apparatus Characterizes Transient Voltages in Real Time

Only the most relevant data are recorded.

*John F. Kennedy Space Center, Florida*

The figure shows a prototype of a relatively inexpensive electronic monitoring apparatus that measures and records selected parameters of lightning-induced transient voltages on communication and power cables. The selected parameters, listed below, are those most relevant to the ability of lightning-induced transients to damage electronic equipment.

This apparatus bridges a gap between some traditional transient-voltage recorders that record complete waveforms and other traditional transient-voltage recorders that record only peak values: By recording the most relevant parameters — and only those parameters — this apparatus yields more useful information than does a traditional peak-value (only) recorder while imposing much smaller data-storage and data-transmission burdens than does a traditional complete-waveform recorder. Also, relative to a complete-waveform

recorder, this apparatus is more reliable and can be built at lower cost because it contains fewer electronic components.

The transients generated by sources other than lightning tend to have frequency components well below 1 MHz. Most commercial transient recorders can detect and record such transients, but cannot respond rapidly enough for recording lightning-induced transient voltage peaks, which can rise from 10 to 90 percent of maximum amplitude in a fraction of a microsecond. Moreover, commercial transient recorders cannot rearm themselves rapidly enough to respond to the multiple transients that occur within milliseconds of each other on some lightning strikes.

One transient recorder, designed for Kennedy Space Center earlier [“Fast Transient-Voltage Recorder” (KSC-11991), *NASA Tech Briefs*, Vol. 23, No. 10, page 6a (October 1999)], is capable of sampling transient voltages at peak val-

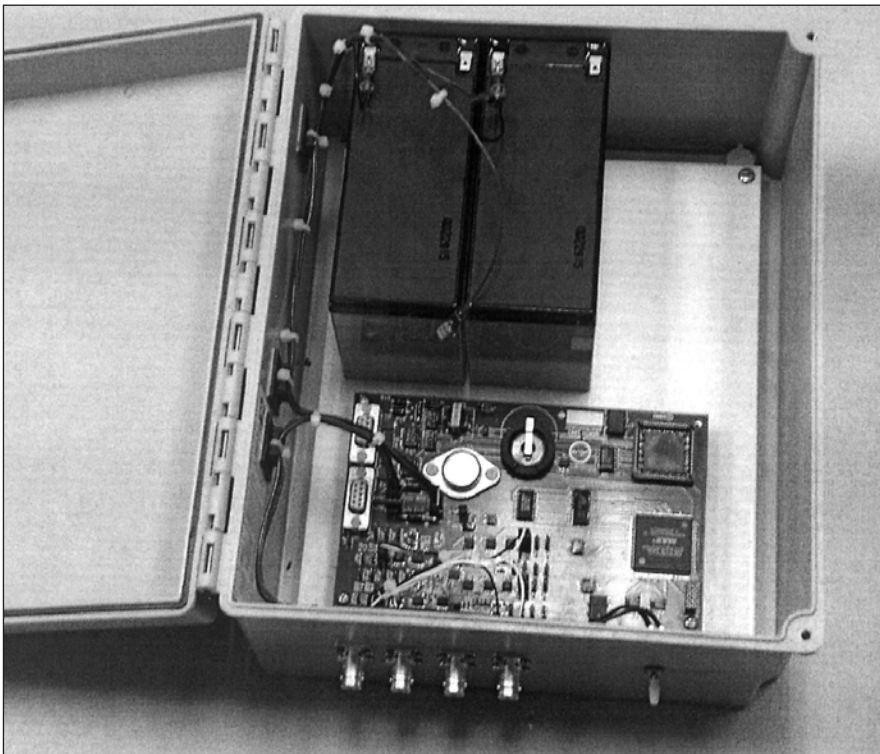
ues up to 50 V in four channels at a rate of 20 MHz. That recorder contains a trigger circuit that continuously compares the amplitudes of the signals on four channels to a preset triggering threshold. When a trigger signal is received, a volatile memory is filled with data for a total time of 200 ms. After the data are transferred to nonvolatile memory, the recorder rearms itself within 400 ms to enable recording of subsequent transients. Unfortunately, the recorded data must be retrieved through a serial communication link. Depending on the amount of data recorded, the memory can be filled before retrieval is completed. Although large amounts of data are recorded and retrieved, only a small part of the information (the selected parameters) is usually required.

The present transient-voltage recorder provides the required information, without incurring the overhead associated with the recording, storage, and retrieval of complete transient-waveform data. In operation, this apparatus processes transient voltage waveforms in real time to extract and record the selected parameters. An analog-to-digital converter that operates at a speed of as much as 100 megasamples per second is used to sample a transient waveform. A real-time comparator and peak detector are implemented by use of fast field-programmable gate arrays.

The parameters extracted from the samples and recorded are the following:

- Peak voltage;
- Duration of each transient at 75 percent of peak voltage, in increments of 10 ns;
- Duration of each transient at 50 percent of peak voltage, in increments of 10 ns;
- Duration of rise from 10 to 90 percent of peak voltage;
- Duration of fall from 90 to 10 percent of peak voltage; and
- Energy content of each transient pulse.

Unlike a traditional complete-waveform recorder, which typically records several thousand bytes per waveform,



This **Prototype Transient-Voltage Recorder** offers high performance, yet the estimated cost of its electronic components is no more than \$200 at 2003 prices.

this apparatus stores fewer than 20 bytes per waveform. The bandwidth needed to transmit the data to a remote recording or control station is reduced correspondingly. In addition, the dead time between subsequent triggers of this apparatus is only about 0.1 ms — less than a hundredth of that of the prior transient recorder.

This transient-voltage recorder can be configured for different input voltage ranges to accommodate the expected magnitudes of the transients to be monitored. Typical input ranges include  $\pm 10$  V,  $\pm 50$  V, and  $\pm 100$  V. The input termination can be either single-ended or differential and selectable among impedances of 50, 120, or 10 kilohms. Either a positive or a negative transient can trigger

sampling, real-time processing, and recording. Depending on the specific setup, data in multiple channels could be analyzed simultaneously, triggered by signal from any one of the channels.

A clock circuit is included to enable accurate time-stamping of any recorded waveform. Time stamping is necessary if a transient measured by this apparatus is to be correlated with measurements by such other apparatuses as a lightning-location system.

The power supply of the transient-voltage recorder includes backup batteries that can maintain operation for as long as 15 days when main AC power is lost. During normal operation when AC power is available, the batteries are charged automatically.

*This work was done by Pedro Medelius of ASRC Aerospace Corp. for Kennedy Space Center. For further information, contact:*

*Lynne R. Henkiel, KSC Industry Liaison  
KSC Technology Programs & Commercialization Office*

*Mail Code YA-C1*

*Kennedy Space Center, FL 32899*

*Phone: (321) 867-8130*

*Fax: (321) 867-2050*

*E-mail: Lynne.Henkiel-1@ksc.nasa.gov*

*This invention is owned by NASA, and a patent application has been filed. Inquiries concerning nonexclusive or exclusive license for its commercial development should be addressed to the Innovative Partnerships Office, Kennedy Space Center, (321) 867-8130. Refer to KSC-12494.*

## Measuring Humidity in Sealed Glass Encasements

**This noninvasive technique helps in the preservation of valuable documents.**

*Langley Research Center, Hampton, Virginia*

A technique has been devised for measuring the relative humidity levels in the protective helium/water vapor atmosphere in which the Declaration of Independence, the United States Constitution, and the Bill of Rights are encased behind glass panels on display at the National Archives in Washington, DC. The technique is noninvasive: it does not involve penetrating the encasements (thereby risking contamination or damage to the priceless documents) to acquire samples of the atmosphere. The technique could also be applied to similar glass encasements used to protect and display important documents and other precious objects in museums.

The basic principle of the technique is straightforward: An encasement is maintained at its normal display or operating temperature (e.g., room temperature) while a portion of its glass front panel is

chilled (see Figure 1) until condensed water droplets become visible on the inside of the panel. The relative humidity of the enclosed atmosphere can then be determined as a known function of the dew point, the temperature below which

the droplets condense.

Notwithstanding the straightforwardness of the basic principle, careful attention to detail is necessary to enable accurate determination of the dew point. In the initial application, the affected por-

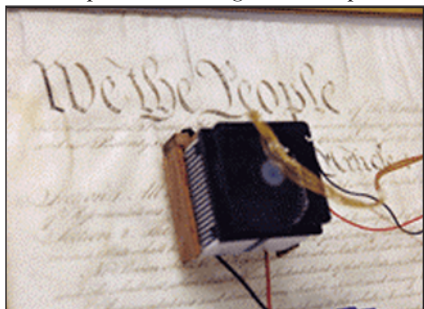


Figure 1. A Thermoelectric Device rests on the encasement.

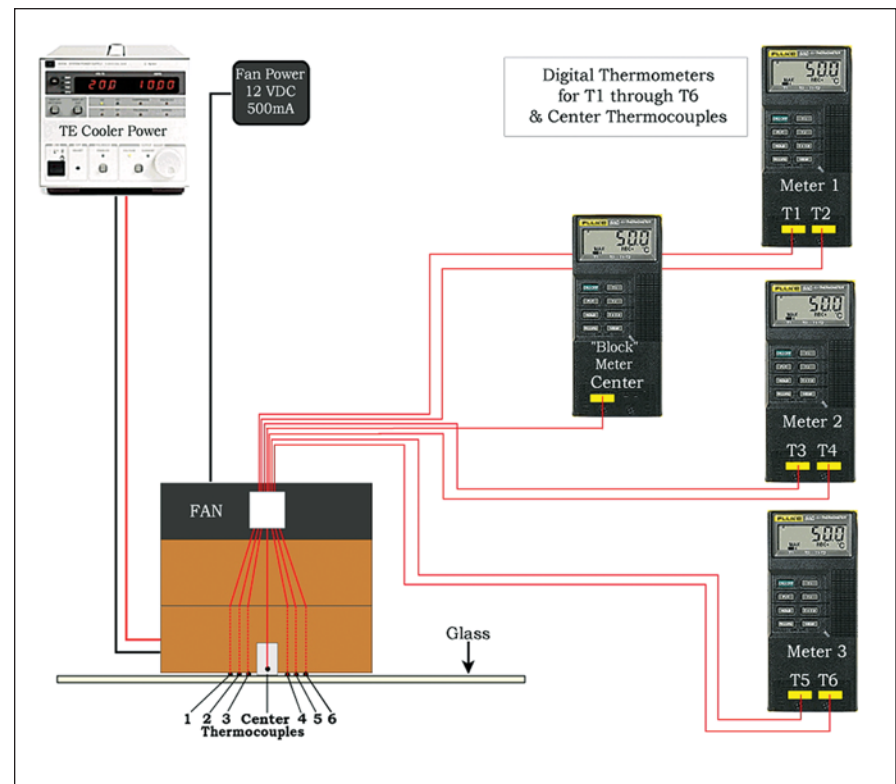


Figure 2. A Thermoelectric Cooler assembly and instrumentation has seven thermocouples to measure temperatures at different locations.

tion of the glass panel was cooled by contact with an aluminum plate that was cooled by a thermoelectric module, the exhaust heat of which was dissipated by a heat sink cooled by a fan. A thermocouple was used to measure the interior temperature of the aluminum plate, and six other thermocouples were used to measure the temperatures at six locations on the cooled outer surface of the glass panel (see Figure 2). Thermal grease was applied to the aluminum plate and the thermocouples to ensure close thermal contact.

Power was supplied to the thermoelec-

tric module in small increments, based on previous laboratory tests. A small flashlight and a magnifying glass were used to look for water droplets condensing on the inner surface of the glass. The temperature readings of the thermocouples were taken during cool-down and upon observing condensation.

In determining the dew point, it was necessary to make a correction for the differences between the temperatures measured on the chilled outer surface of the glass and the temperature of the inner surface, where the condensation took place. The correction was derived

from a laboratory test on a measurement setup that was nearly identical, except that the dew location on the inner surface was also instrumented with a thermocouple. The test showed that the temperature at the dew location on the inner surface of the glass panel was 0.9 C° above the temperature determined from the measurements on the chilled outer surface of the panel.

*This work was done by James W. West, Cecil G. Burkett, and Joel S. Levine of Langley Research Center. Further information is contained in a TSP (see page 1). LAR-16422-1*

## Adaptable System for Vehicle Health and Usage Monitoring

Safety can be increased, while costs and downtime can be reduced.

Langley Research Center, Hampton, Virginia

Aircraft and other vehicles are often kept in service beyond their original design lives. As they age, they become susceptible to system malfunctions and fatigue. Unlike future aircraft that will include health-monitoring capabilities as integral parts in their designs, older aircraft have not been so equipped.

The Adaptable Vehicle Health and Usage Monitoring System is designed to be retrofitted into a preexisting fleet of military and commercial aircraft, ships, or ground vehicles to provide them with state-of-the-art health- and usage-monitoring capabilities. The monitoring system is self-contained, and the integration of it into existing systems entails limited intrusion. In essence, it has “bolt-on/bolt-off” simplicity that makes it easy to install on any preexisting vehicle or structure. Because the system is completely

independent of the vehicle, it can be certified for airworthiness as an independent system.

The purpose served by the health-monitoring system is to reduce vehicle operating costs and to increase safety and reliability. The monitoring system is a means to identify damage to, or deterioration of, vehicle subsystems, before such damage or deterioration becomes costly and/or disastrous. Frequent monitoring of a vehicle enables identification of the embryonic stages of damage or deterioration. The knowledge thus gained can be used to correct anomalies while they are still somewhat minor. Maintenance can be performed as needed, instead of having the need for maintenance identified during cyclic inspections that take vehicles off duty even when there are no maintenance problems. Measurements and analyses ac-

quired by the health-monitoring system also can be used to analyze mishaps. Overall, vehicles can be made more reliable and kept on duty for longer times.

Figure 1 schematically depicts the system as applied to a fleet of  $n$  vehicles. The system has three operational levels. All communication between system components is by use of wireless transceivers operating at frequencies near 433 MHz. Electromagnetic-interference tests have demonstrated that the radio-frequency emissions from the transceivers do not influence civilian

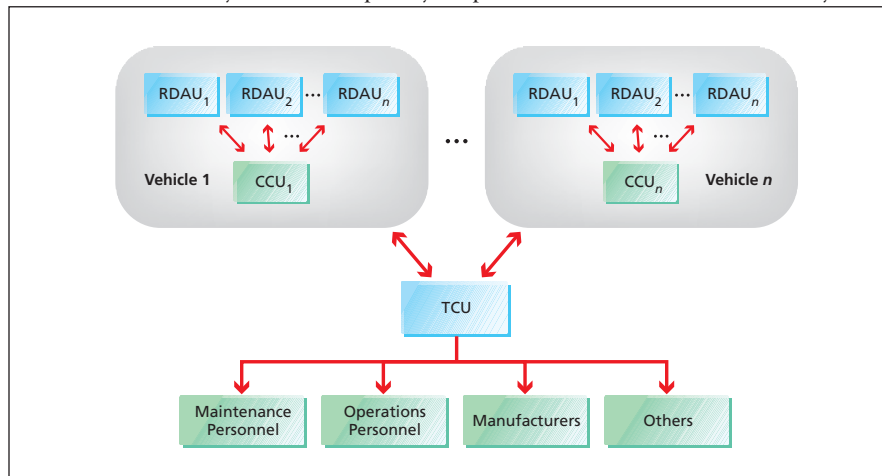


Figure 1. The Adaptable Vehicle Health and Usage Monitoring System is characterized by three levels of operation and analysis.



Figure 2. An RDAU Mounted on a Landing Gear was used to perform a rigorous test of the system.

aircraft communication and navigation systems.

The first level of the system includes one or more remote data-acquisition units (RDAUs) placed at different locations within each aircraft or other vehicle. An RDAU acquires, stores, and analyzes sensor data. The user has the capability to define the number of inputs, type of sensors, sensor input characteristics, aggregate sampling rate, and acquisition period duration. This information is used to configure the sampling interface and its associated multiplexed eight-channel analog-to-digital converter. An RDAU can analyze measurements from each channel individually or from all channels fused together. Programmable data-acquisition circuitry and expert-system software trained to performance baselines in each RDAU make it possible to adapt the system to many types of vehicles and structures. The RDAU has been tested at temperatures from  $-50$  to  $+55$  °C. Pressure testing has verified that RDAUs could be used in non-environmentally-controlled spaces on aircraft at altitudes up to 50,000 ft (15.24 km). Vibration tests have verified that RDAUs can operate during vibrations representative of those of commercial aircraft. The final vibrations used in the tests had an amplitude of 20 times normal Earth gravitational acceleration and a frequency of 2 kHz.

The second level of the system includes a command-and-control unit (CCU) in each

vehicle. The CCU regulates the health-monitoring activities in the vehicle. The CCU is a computer-based subsystem that controls communications to and from all RDAUs; regulates all RDAU measurement, collection, and analysis; and retrieves the results of all data-collection and analysis performed by the RDAUs.

The third level of the system is a terminal collection unit (TCU). The TCU provides the means to autonomously retrieve vehicle analysis results from all the CCUs or RDAUs of all vehicles. The TCU analyzes all results collected from all vehicles to identify any fleet-wide anomalies (e.g., all aircraft have the same faulty bearing at a similar location). The TCU is used to develop the final summary of the vehicle health. The summary is routed to the appropriate users (e.g., maintenance workers and airline operations personnel).

The system can also serve as an infrastructure for performing tributary analyses: NASA Langley Research Center has developed a parameterized fuzzy expert-system algorithm that can be trained to a user's subjective analysis of data. The expert-system algorithm and other analysis algorithms can be used at each operational level. The measurements collected at the lowest level can be analyzed at that level. Analysis results are forwarded to next operational level, and then all results are analyzed to ascertain global trends or anomalies for the prior level. This is repeated until all analyses

are combined at the hierarchically highest level (e.g., the third level).

The trainable parameterized fuzzy expert system, the wireless communication between components, and the programmable digital interface make the health-monitoring hardware and software infrastructure adaptable to many vehicles and structures. Performing analysis at each level eliminates the need for transmitting and storing large volumes of collected measurements.

The RDAU hardware and the non-analytical portion of the software of the system have been flight-tested on the landing gear of Langley Research Center's Boeing 757 airplane (see Figure 2) — the most severe location on that airplane for mounting a health-monitoring device. During test flights, the CCU was located in the passenger section of the airplane. A portable TCU equipped with the non-analytical capabilities of the TCU was shown to function as intended in downloading of data after flights.

*This work was done by Stanley E. Woodart, Keith L. Woodman, and Neil C. Coffey of Langley Research Center and Bryant D. Taylor of Swales Corp. Further information is contained in a TSP (see page 1).*

*This invention is owned by NASA, and a patent application has been filed. Inquiries concerning nonexclusive or exclusive license for its commercial development should be addressed to the Patent Counsel, Langley Research Center, at (757) 864-3521. Refer to LAR-16516.*

## Miniature Focusing Time-of-Flight Mass Spectrometer

Resolution is retained despite the reduction in size.

NASA's Jet Propulsion Laboratory, Pasadena, California

An improved miniature time-of-flight mass spectrometer has been developed in a continuing effort to minimize the sizes, weights, power demands, and costs of mass spectrometers for such diverse applications as measurement of concentrations of pollutants in the atmosphere, detecting poisonous gases in mines, and analyzing exhaust gases of automobiles. Advantageous characteristics of this mass spectrometer include the following:

- It is simple and rugged.
- Relative to prior mass spectrometers, it is inexpensive to build.
- There is no need for precise alignment of its components.
- Its mass range is practically unlimited.

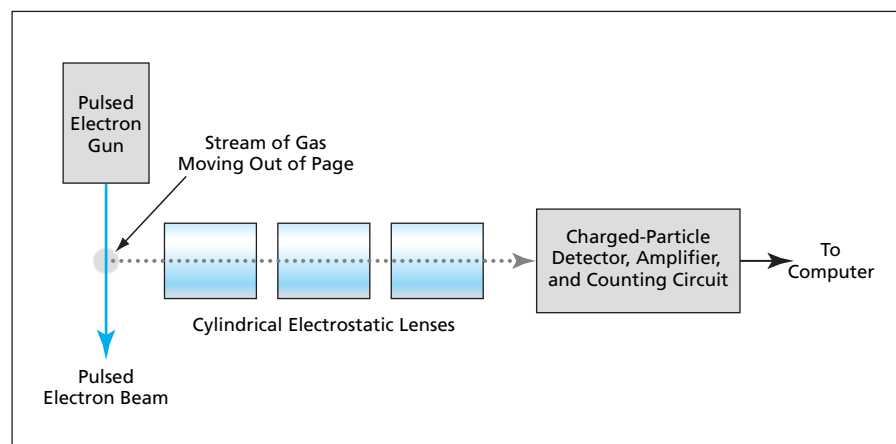


Figure 1. This Miniature Time-of-Flight Mass Spectrometer utilizes charged-particle optics in conjunction with ion speeds smaller than those of similar prior instruments.

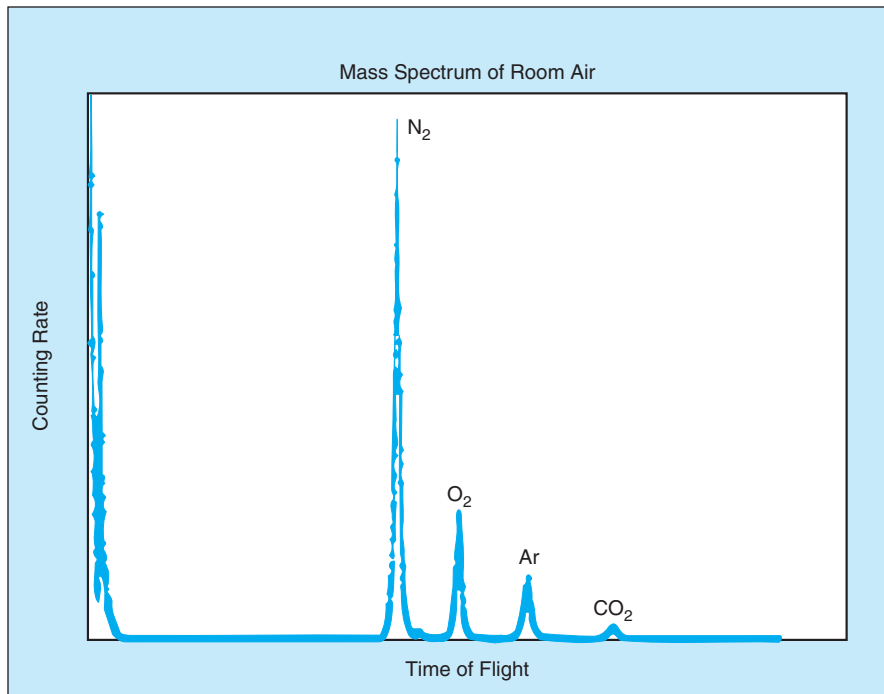


Figure 2. This **Uncalibrated Mass Spectrum** of air was acquired by use of the improved TOF-MS.

- Relative to prior mass spectrometers, it offers high sensitivity (ability to measure relative concentrations as small as parts per billion).
- Its resolution is one dalton (one atomic mass unit).
- An entire mass spectrum is recorded in a single pulse. (In a conventional mass

spectrometer, a spectrum is recorded mass by mass.) The data-acquisition process takes only seconds.

- It is a lightweight, low-power, portable instrument.

Although time-of-flight mass spectrometers (TOF-MSs) have been miniaturized previously, their performances

have not been completely satisfactory. An inherent adverse effect of miniaturization of a TOF-MS is a loss of resolution caused by reduction of the length of its flight tube. In the present improved TOF-MS, the adverse effect of shortening the flight tube is counteracted by (1) using charged-particle optics to constrain ion trajectories to the flight-tube axis while (2) reducing ion velocities to increase ion flight times.

In the present improved TOF-MS, a stream of gas is generated by use of a hypodermic needle. The stream of gas is crossed by an energy-selected, pulsed beam of electrons (see Figure 1). The ions generated by impingement of the electrons on the gas atoms are then focused by three cylindrical electrostatic lenses, which constitute a segmented flight tube. After traveling along the flight tube, the ions enter a charged-particle detector. The output of the detector is fed to a counting circuit to obtain data on the counting rate as a function of time. Inasmuch as time of flight is directly proportional to the ion mass, a plot of the counting rate versus time of flight is equivalent to a mass spectrum (see Figure 2).

*This work was done by Isik Kanik and Santosh Srivastava of Caltech for NASA's Jet Propulsion Laboratory. Further information is contained in a TSP (see page 1) NPO-30611*

## Cryogenic High-Sensitivity Magnetometer

Sensitivity would be about a million times that of a flux-gate magnetometer.

NASA's Jet Propulsion Laboratory, Pasadena, California

A proposed magnetometer for use in a cryogenic environment would be sensitive enough to measure a magnetic-flux density as small as a picogauss ( $10^{-16}$  Tesla). In contrast, a typical conventional flux-gate magnetometer cannot measure a magnetic-flux density smaller than about 1 microgauss ( $10^{-10}$  Tesla).

One version of this device, for operation near the low end of the cryogenic temperature range, would include a piece of a paramagnetic material on a platform, the temperature of which would be controlled with a periodic variation. The variation in temperature would be measured by use of a conventional germanium resistance thermometer. A superconducting coil would be wound around the paramagnetic material and coupled to a superconducting

quantum interference device (SQUID) magnetometer.

The SQUID magnetometer would be used to measure the change in current in the coil as a result of the change in temperature measured by the germanium resistance thermometer. The ratio between the current change and the temperature change would be computed, then used to infer the ambient magnetic field. This inference would be drawn from a lookup table established by prior calibration measurements performed at the same mean operating temperature.

In an alternative version of this magnetometer, for operation at a temperature near the high end of the cryogenic range, the coil and the SQUID magnetometer would be made from a high-temperature superconductor and the

coil would be in the form of a thin film deposited on the same substrate as that of the SQUID. The paramagnetic material would be inserted in a hole at the center of the coil. The temperature of the whole substrate would then be modulated during measurements of the type described above.

Because of the oscillatory temperature excitation, this magnetometer would exhibit very little drift. The highest sensitivity and the lowest noise would be achieved by careful selection of the paramagnetic material and operating near the Curie temperature of that material.

Although the SQUID magnetometer and the superconducting coil must be kept cold, it would be possible to measure the magnetic field of a warm environment. For this purpose, the magne-

tometer could be kept at the required low temperature in a nonmagnetic Dewar flask, which could be brought to the warm measurement location.

While conventional SQUID magnetometers are routinely used to measure the change in magnetic flux density with similar sensitivity, the proposed implementation allows the full sensitivity of

SQUID to be used to measure a small static magnetic flux density. Another implementation method involves flipping the pickup coil of a SQUID to measure the ambient static field. Although such a method had been used before, it involves cumbersome mechanical actuators to flip the coil at cryogenic temperatures and the wire of the coil can work

harden and break after repeated flipping. Because of the absence of moving parts in the proposed magnetometer, reliability is improved.

*This work was done by Peter Day, Talso Chui, and David Goodstein of Caltech for NASA's Jet Propulsion Laboratory. Further information is contained in a TSP (see page 1). NPO-40748*

---

## Wheel Electrometer System

*John F. Kennedy Space Center, Florida*

Two documents describe a prototype system of electrometers for measuring electrostatic fields and electrostatic responses of soils on Mars and the Moon. The electrodes of this electrometer are embedded in a wheel of an exploratory robotic vehicle, utilizing the wheel motion to bring the electrodes into proximity or contact with the soil. Each electrode resides in one of two types of sensor modules: electric-field (ELF) or triboelectric (TRIBO). In either type, what is measured is simply the electric

charge induced on the electrode by exposure to the external distribution of electrostatic charge. In an ELF module, the electrode is bare and recessed radially from the wheel surface. The ELF sensor provides a measure of the charge on a small patch of undisturbed soil as the wheel rolls forward. In a TRIBO module, the electrode is only slightly recessed and covered with a polymeric insulator flush with the wheel surface. Through contact electrification, the insulator exchanges charge with the soil. There are five

TRIBO sensors, each containing an insulator made of a different polymer. The charge data gathered by the five TRIBO sensors can be used to determine how the soil fits into a triboelectric series.

*This work was done by Carlos I. Calle of Kennedy Space Center, Martin G. Buehler of NASA's Jet Propulsion Laboratory, James G. Mantovani (an independent contractor), and Charles R. Buhler and Andrew Nowicki of Arctic Slope Research Corp. Further information is contained in a TSP (see page 1). KSC-12677*



## Carbon-Nanotube Conductive Layers for Thin-Film Solar Cells

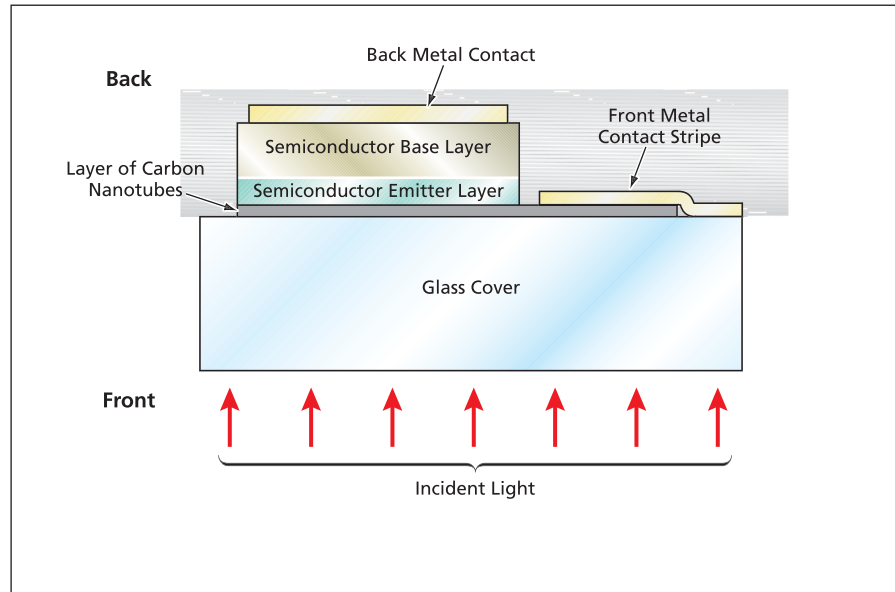
Energy-conversion efficiencies could be increased.

John H. Glenn Research Center, Cleveland, Ohio

Thin, transparent layers comprising mats of carbon nanotubes have been proposed for providing lateral (that is, in-plane) electrical conductivities for collecting electric currents from the front surfaces of the emitter layers of thin-film solar photovoltaic cells. Traditionally, thin, semitransparent films of other electrically conductive materials (usually, indium tin oxide, zinc oxide, or cadmium sulfide) have been used for this purpose. As in the cases of the traditional semitransparent conductive films, the currents collected by the nanotube layers would, in turn, be further collected by front metal contact stripes.

Depending on details of a specific solar-cell design, the layer of carbon nanotubes would be deposited in addition to, or instead of, a semitransparent conductive layer of one of these traditional conductive materials (see figure). The proposal is expected to afford the following advantages:

- The electrical conductivity of the carbon-nanotube layer would exceed that of the corresponding semitransparent layer of traditional electrically conductive material.
- The greater electrical conductivity of the carbon-nanotube layer would make it possible to retain adequate lateral electrical conductivity while reducing the thickness of, or eliminating entirely, the traditional semitransparent conductive layer. As a consequence of thinning or elimination of the traditional semitransparent conductive layer, less light would be absorbed, so that more of the incident light would be available for photovoltaic conversion.
- The greater electrical conductivity of the carbon-nanotube layer would make it possible to increase the distance between front metal contact stripes, in addition to (or instead of) thinning or eliminating the layer of traditional semitransparent conductive material. Consequently, the fraction of solar-cell area shadowed by front metal contact stripes would be reduced — again, making more of the incident light available for photovoltaic conversion.



A **Layer of Carbon Nanotubes** — instead of a traditional layer of indium tin oxide, zinc oxide, or cadmium sulfide — would conduct electric current from the front surface of the emitter layer to the front metal contact stripe.

- The electrical conductivities of individual carbon nanotubes can be so high that the mat of carbon nanotubes could be made sparse enough to be adequately transparent while affording adequate lateral electrical conductivity of the mat as a whole. The thickness of the nanotube layer would be chosen so that the layer would contribute significant lateral electrical conductivity, yet would be as nearly transparent as possible to incident light. A typical thickness for satisfying these competing requirements is expected to lie between 50 and 100 nm. The optimum thickness must be calculated by comparing the lateral electrical conductivity, the distance between front metal stripes, and the amount of light lost by absorption in the nanotube layer.

The diameters of carbon nanotubes — of the order of 10 nm — are smaller than the typical wavelengths of the light absorbed by solar cells. Carbon nanotubes can be made in either highly conductive “metallic” form or in a semiconducting form; for the present purpose, the highly conductive form would

be best. Most preferable would be single-wall carbon nanotubes, which have the smallest diameters. It would also be preferable to align all the carbon nanotubes parallel to the desired direction of conduction, but such alignment may be difficult to achieve at low cost. Even without such alignment, it should be possible to attain adequate lateral electrical conductivity.

During fabrication, the layer of carbon nanotubes could be deposited (e.g., from a liquid suspension) onto either the front surface of the solar-cell emitter layer or on the glass cover prior to attachment of the cover by use of an adhesive. In either case the carbon nanotubes would adhere to the deposition surface by means of van der Waals forces.

*This work was done by Geoffrey A. Landis of Glenn Research Center. Further information is contained in a TSP (see page 1).*

*Inquiries concerning rights for the commercial use of this invention should be addressed to NASA Glenn Research Center, Innovative Partnerships Office, Attn: Steve Fedor, Mail Stop 4-8, 21000 Brookpark Road, Cleveland, Ohio 44135. Refer to LEW-17562/3-1.*

---

## Patch Antenna Fed via Unequal-Crossed-Arm Aperture

The antenna could be made significantly smaller in one dimension.

NASA's Jet Propulsion Laboratory, Pasadena, California

A proposed rectangular-patch antenna for transmitting or receiving microwave circularly polarized (CP) radiation would be fed via a cross-shaped aperture that would have unequal arms and would, in turn, be fed at a single point via a microstrip transmission line. As a consequence of the unequal-arm aperture design, the antenna could be made smaller in one dimension, relative to a typical prior CP antenna that comprises a nearly square patch fed via an equal-crossed-arm aperture. Hence, in designing a phased array of such antennas, the antennas could be packed together more closely along one dimension, making it possible to scan the beam radiated by the antenna over a wider angular range in a plane that includes that dimension. Alternatively or in addition, one could lay out transmission lines in the extra spaces created by the shortening in one dimension.

In designing a rectangular-patch CP antenna, one chooses the dimensions of the patch and of the crossed arms of the aperture to introduce a 90° phase shift between the two orthogonal electromagnetic modes of the patch. In the case of a conventional

“nearly square” design, the aperture arms are constrained to have equal dimensions, it is assumed that the value of the resonance quality factor ( $Q$ ) is the same for both modes, and the effects of the electromagnetic modes of the crossed aperture arms are neglected. In designing an antenna according to the proposal, one allows the aperture arms to have unequal dimensions and does not assume equal  $Q$  values. Instead, one explicitly includes the aperture modes in the calculations and assesses the overall effects (including possibly unequal  $Q$  values) on the patch modes and the characteristics of the radiation.

The decision to allow unequal dimensions of both the patch and the aperture arms gives the designer more degrees of freedom than could be utilized to optimize the antenna. Among other things that one seeks to do in optimization is to obtain an axial ratio as close to 1 as possible and an axial-ratio bandwidth as large as possible. (As used here, “axial ratio” signifies the ratio between the radiated power polarized along one axis of symmetry of the antenna and the radiated power polarized along the other, perpen-

dicular axis of symmetry of the antenna. An axial ratio of exactly 1 corresponds to perfectly circular polarization. “Axial-ratio bandwidth” signifies the width of the frequency band over which the axial ratio is acceptably close to 1.)

In designing an antenna as proposed, to compensate for an axial ratio that deviates from 1 by an unacceptably large amount, the dimensions of the aperture arms along one direction could be adjusted in tandem with the corresponding orthogonal patch dimension. For example, if the vertical dimension of the patch were modified, then the horizontal dimensions of the aperture arms would be adjusted accordingly. Consequently, an additional benefit of the proposed design approach would be that the axial ratio of an antenna would be closer to 1, and the axial-ratio bandwidth would be greater, relative to the corresponding parameters of the prior “nearly square” antenna.

*This work was done by Larry Epp of Caltech for NASA's Jet Propulsion Laboratory. Further information is contained in a TSP (see page 1).  
NPO-30508*

---

## LC Circuits for Diagnosing Embedded Piezoelectric Devices

Failures are readily identified through changes in resonance frequencies.

Langley Research Center, Hampton, Virginia

A recently invented method of non-intrusively detecting faults in piezoelectric devices involves measurement of the resonance frequencies of inductor-capacitor (LC) resonant circuits. The method is intended especially to enable diagnosis of piezoelectric sensors, actuators, and sensor/actuators that are embedded in structures and/or are components of multilayer composite-material structures.

In this method, a small induction coil is connected to each piezoelectric component that is embedded in the affected structure, composite material, or component by way of the electrical leads used for the basic sensor/actuator function. This connection is made manually or remotely during diagnosis of the piezoelectric component. Thus, what is formed, in addition to the basic

sensor/actuator circuit, is an LC resonant circuit, in which the piezoelectric component acts as the capacitor. The inductance of the coil does not vary appreciably under most conditions, but the capacitance (and, hence, the resonance frequency) changes significantly if the piezoelectric device fails. Hence, a significant change in the resonance frequency can be taken as an indication of a failure of the piezoelectric device.

The resonance frequency can be measured in a conventional manner, either by induction or by direct connection via electrical leads. If a structure contains multiple embedded piezoelectric devices and the LC circuit of each piezoelectric device has a unique assigned resonance frequency, then one can rapidly and easily interrogate all

the devices in a spectral scan over the range of assigned resonance frequencies. In the resulting spectral plot, a significant deviation of any of the resonance peaks from its assigned frequency indicates the failure of the corresponding piezoelectric device.

*This work was done by Richard L. Chaitin, Robert Lee Fox, Robert W. Moses, and Qamar A. Shams of Langley Research Center. For further information, access the Technical Support Package (TSP) free online at [www.techbriefs.com/tsp](http://www.techbriefs.com/tsp) under the Semiconductors & ICs category.*

*This invention is owned by NASA, and a patent application has been filed. Inquiries concerning nonexclusive or exclusive license for its commercial development should be addressed to the Patent Counsel, Langley Research Center, at (757) 864-3521. Refer to LAR-16549-1.*



# Nanowire Thermoelectric Devices

Efficiencies would be considerably greater than those of conventional thermoelectric devices.

NASA's Jet Propulsion Laboratory, Pasadena, California

Nanowire thermoelectric devices, now under development, are intended to take miniaturization a step beyond the prior state of the art to exploit the potential advantages afforded by shrinking some device features to approximately molecular dimensions (of the order of 10 nm). The development of nanowire-based thermoelectric de-

vices could lead to novel power-generating, cooling, and sensing devices that operate at relatively low currents and high voltages.

Recent work on the theory of thermoelectric devices has led to the expectation that the performance of such a device could be enhanced if the diameter of the wires could be reduced to a point

where quantum confinement effects increase charge-carrier mobility (thereby increasing the Seebeck coefficient) and reduce thermal conductivity. In addition, even in the absence of these effects, the large aspect ratios (length of the order of tens of microns  $\div$  diameter of the order of tens of nanometers) of nanowires would be conducive to the maintenance of large temperature differences at small heat fluxes. The predicted net effect of reducing diameters to the order of tens of nanometers would be to increase its efficiency by a factor of  $\approx 3$ .

Nanowires made of thermoelectric materials and devices that comprise arrays of such nanowires can be fabricated by electrochemical growth of the thermoelectric materials in templates that contain suitably dimensioned pores (10 to 100 nm in diameter and 1 to 100  $\mu\text{m}$  long). The nanowires can then be contacted in bundles to form devices that look similar to conventional thermoelectric devices, except that a production version may contain nearly a billion elements (wires) per square centimeter, instead of fewer than a hundred as in a conventional bulk thermoelectric device or fewer than 100,000 as in a microdevice.

It is not yet possible to form contacts with individual nanowires. Therefore, in fabricating a nanowire thermoelectric device, one forms contacts on nanowires in bundles of the order of 10- $\mu\text{m}$  wide. The fill factor for the cross-section of a typical bundle is about 1/2. Nanowires have been grown in alumina templates with pore diameters of 100 and 40 nm. To ensure that every pore in a template is filled with a nanowire, one allows the thermoelectric material to grow onto the top of the template (see Figure 1), then polishes the template back to a level where every pore is filled.

After polishing, contacts on bundles of nanowires can be made by electrochemical deposition of nickel or another suitable metal. Figure 2 depicts a proposed configuration for growing bundles of n- and p-type nanowires, electrically connecting the wires of each bundle in parallel, and electrically connecting successive bundles in series to make a thermoelectric device. The bundles would be suitably masked to allow

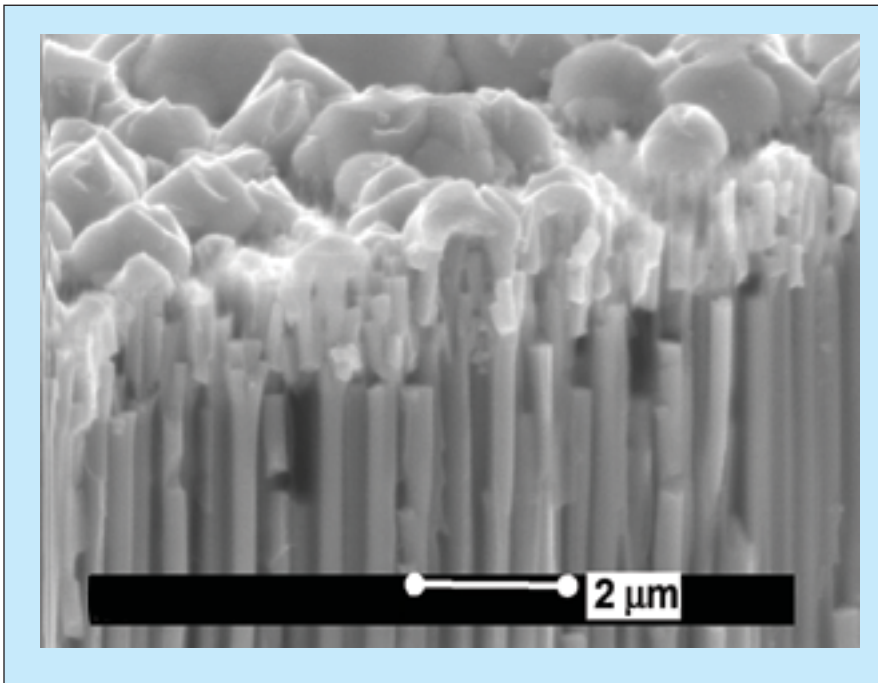


Figure 1. Thermoelectric Nanowires of n-Type  $\text{Bi}_2\text{Te}_3$  with a diameter of 10 nm and length of 40  $\mu\text{m}$  were grown in an alumina template. The thermoelectric material was allowed to grow onto the top of the template, forming caps that make contact with each other. In a production version, the overgrowth and part of the template would be polished away and metal contacts deposited as in Figure 2.

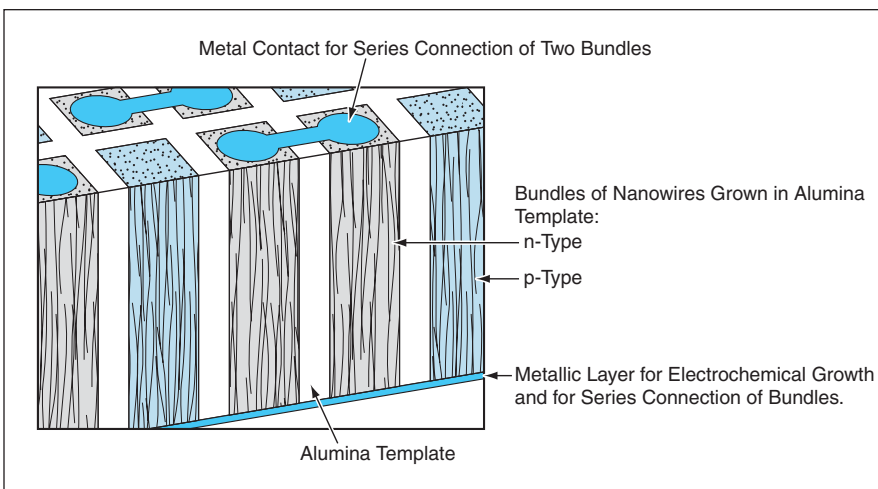


Figure 2. Bundles of Nanowires would be grown electrochemically in an alumina template. The nanowires in each bundle would be electrically connected in parallel and the bundles electrically connected in series by metal contacts grown electrochemically on the ends of the bundles.

electrochemical growth only in the desired areas. For a given bundle, the metal caps would be made to electrochemically grow out from the exposed ends of the nanowires, eventually merging to form one metal contact.

*This work was done by Alexander Borshchevsky, Jean-Pierre Fleurial, Jennifer Herman, and Margaret Ryan of Caltech for*

**NASA's Jet Propulsion Laboratory.** *Further information is contained in a TSP (see page 1).*

*In accordance with Public Law 96-517, the contractor has elected to retain title to this invention. Inquiries concerning rights for its commercial use should be addressed to:*

*Innovative Technology Assets Management  
JPL*

*Mail Stop 202-233  
4800 Oak Grove Drive  
Pasadena, CA 91109-8099  
(818) 354-2240*

*E-mail: [iaoffice@jpl.nasa.gov](mailto:iaoffice@jpl.nasa.gov)  
Refer to NPO-30210, volume and number of this NASA Tech Briefs issue, and the page number.*

### Code for Analyzing and Designing Spacecraft Power System Radiators

GPHRAD is a computer code for analysis and design of disk or circular-sector heat-rejecting radiators for spacecraft power systems. A specific application is for Stirling-cycle/linear-alternator electric-power systems coupled to radioisotope general-purpose heat sources. GPHRAD affords capabilities and options to account for thermophysical properties (thermal conductivity, density) of either metal-alloy or composite radiator materials. GPHRAD also enables specification of a heat-pipe radiator design with a radial location of the embedded heat-pipe condenser section determined numerically so that minimum radiator area is obtained. Alternatively, the user can specify a radial location of the heat-pipe condenser section for easier assembly with other components. In this case, GPHRAD determines the tradeoff cost in increased radiator area for this choice. A third option is to design a radiator without heat pipes, with heat flowing radially outward from the cylindrical cold section of the Stirling power system. A major subroutine, TSCALC, calculates an equilibrium sink temperature for a radiator, taking account of the solar absorptivity and thermal emissivity of the radiator surface, the spacecraft-to-Sun distance expressed in astronomical units (AU), the angle at which solar radiation is incident on the radiator surface, and the view factor to space of the radiator surface and the infrared absorptivity-to-emissivity ratio for planetary thermal radiation, if any. The sink temperature, along with the heat-source temperature and properties of the radiator material, serve as inputs to the GPHRAD code, which then calculates dimensions of, and temperature distribution within the radiator for a required heat-rejection load at given heat-rejection source temperature, such as the Stirling power system “cold” side temperature. The option to specify the disk tip-to-hub thickness ratio permits investigation of mass savings achieved by trapezoidal or parabolic tapering of the disk radiator design.

*This program was written by Albert Juhasz of Glenn Research Center. Further information is contained in a TSP (see page 1).*

*Inquiries concerning rights for the commercial use of this invention should be addressed to NASA Glenn Research Center, Innovative Partnerships Office, Attn: Steve Fedor, Mail Stop 4-8, 21000 Brookpark Road, Cleveland, Ohio 44135. Refer to LEW-17053-1.*

### Decision Support for Emergency Operations Centers

The Flood Disaster Mitigation Decision Support System (DSS) is a computerized information system that allows regional emergency-operations government officials to make decisions regarding the dispatch of resources in response to flooding. The DSS implements a real-time model of inundation utilizing recently acquired lidar elevation data as well as real-time data from flood gauges, and other instruments within and upstream of an area that is or could become flooded. The DSS information is updated as new data become available. The model generates real-time maps of flooded areas and predicts flood crests at specified locations. The inundation maps are overlaid with information on population densities, property values, hazardous materials, evacuation routes, official contact information, and other information needed for emergency response. The program maintains a database and a Web portal through which real-time data from instrumentation are gathered into the database. Also included in the database is a geographic information system, from which the program obtains the overlay data for areas of interest as needed. The portal makes some portions of the database accessible to the public. Access to other portions of the database is restricted to government officials according to various levels of authorization. The Flood Disaster Mitigation DSS has been integrated into a larger DSS named REACT (Real-time Emergency Action Coordination Tool), which also provides emergency operations managers with data for any type of impact area such as floods, fires, bomb emergencies, and the like.

*This program was written by Craig Harvey, Joel Lawhead, and Zack Watts of NVision Solutions, Inc., for Stennis Space Center.*

*In accordance with Public Law 96-517, the contractor has elected to retain title to this*

*invention. Inquiries concerning rights for its commercial use should be addressed to:*

*NVision Solutions  
147c Building 1103  
Stennis Space Center, MS 39529  
Phone: (228) 688-2205  
E-mail: info@nvs-inc.com*

*Refer to SSC-00206-1, volume and number of this NASA Tech Briefs issue, and the page number.*

### NASA Records Database

The NASA Records Database, comprising a Web-based application program and a database, is used to administer an archive of paper records at Stennis Space Center. The system begins with an electronic form, into which a user enters information about records that the user is sending to the archive. The form is “smart”: it provides instructions for entering information correctly and prompts the user to enter all required information. Once complete, the form is digitally signed and submitted to the database. The system determines which storage locations are not in use, assigns the user’s boxes of records to some of them, and enters these assignments in the database. Thereafter, the software tracks the boxes and can be used to locate them. By use of search capabilities of the software, specific records can be sought by box storage locations, accession numbers, record dates, submitting organizations, or details of the records themselves. Boxes can be marked with such statuses as checked out, lost, transferred, and destroyed. The system can generate reports showing boxes awaiting destruction or transfer. When boxes are transferred to the National Archives and Records Administration (NARA), the system can automatically fill out NARA records-transfer forms. Currently, several other NASA Centers are considering deploying the NASA Records Database to help automate their records archives.

*This program was written by Christopher Callac and Michelle Lunsford of Lockheed Martin Corp. for Stennis Space Center.*

*Inquiries concerning rights for the commercial use of this invention should be addressed to the Intellectual Property Manager, Stennis Space Center, (228) 688-1929. Refer to SSC-00195.*

---

## ➤ Real-Time Principal-Component Analysis

A recently written computer program implements dominant-element-based gradient descent and dynamic initial learning rate (DOGEDYN), which was described in “Method of Real-Time Principal-Component Analysis” (NPO-40034) *NASA Tech Briefs*, Vol. 29, No. 1 (January 2005), page 59. To recapitulate: DOGEDYN is a method of sequential principal-component analysis (PCA) suitable for such applications as data compression and extraction of features from sets of data. In DOGEDYN, input data are represented as a sequence of vectors acquired at sampling times. The learning algorithm in DOGEDYN involves sequential extraction of principal vectors by means of a gradient descent in which only the dominant element is used at each iteration. Each iteration includes updating of elements of a weight matrix by amounts proportional to a dynamic initial learning rate chosen to increase the rate of convergence by compensating for the energy lost through the previous extraction of principal components. In comparison with a prior method of gra-

dient-descent-based sequential PCA, DOGEDYN involves less computation and offers a greater rate of learning convergence. The sequential DOGEDYN computations require less memory than would parallel computations for the same purpose. The DOGEDYN software can be executed on a personal computer.

*This program was written by Vu Duong and Tuan Duong of Caltech for NASA’s Jet Propulsion Laboratory. Further information is contained in a TSP (see page 1).*

*This software is available for commercial licensing. Please contact Karina Edmonds of the California Institute of Technology at (818) 393-2827. Refer to NPO-40056.*

---

## ➤ Fuzzy/Neural Software Estimates Costs of Rocket-Engine Tests

The Highly Accurate Cost Estimating Model (HACEM) is a software system for estimating the costs of testing rocket engines and components at Stennis Space Center. HACEM is built on a foundation of adaptive-network-based fuzzy inference systems (ANFIS) — a hybrid software concept that combines the adaptive

capabilities of neural networks with the ease of development and additional benefits of fuzzy-logic-based systems. In ANFIS, fuzzy inference systems are trained by use of neural networks. HACEM includes selectable subsystems that utilize various numbers and types of inputs, various numbers of fuzzy membership functions, and various input-preprocessing techniques. The inputs to HACEM are parameters of specific tests or series of tests. These parameters include test type (component or engine test), number and duration of tests, and thrust level(s) (in the case of engine tests). The ANFIS in HACEM are trained by use of sets of these parameters, along with costs of past tests. Thereafter, the user feeds HACEM a simple input text file that contains the parameters of a planned test or series of tests, the user selects the desired HACEM subsystem, and the subsystem processes the parameters into an estimate of cost(s).

*This program was written by Freddie Douglas of Stennis Space Center and Edit Kaminsky Bourgeois of the University of New Orleans.*

*Inquiries concerning rights for the commercial use of this invention should be addressed to the Intellectual Property Manager, Stennis Space Center, (228) 688-1929. Refer to SSC-00194.*



## **Multicomponent, Rare-Earth-Doped Thermal-Barrier Coatings**

**Thermal conductivities are reduced while maximum use temperatures are increased.**

*John H. Glenn Research Center, Cleveland, Ohio*

Multicomponent, rare-earth-doped, perovskite-type thermal-barrier coating materials have been developed in an effort to obtain lower thermal conductivity, greater phase stability, and greater high-temperature capability, relative to those of the prior thermal-barrier coating material of choice, which is yttria-partially stabilized zirconia. As used here, "thermal-barrier coatings" (TBCs) denotes thin ceramic layers used to insulate air-cooled metallic components of heat engines (e.g., gas turbines) from hot gases. These layers are generally fabricated by plasma spraying or physical vapor deposition of the TBC materials onto the metal components.

A TBC as deposited has some porosity, which is desirable in that it reduces the thermal conductivity below the intrinsic thermal conductivity of the fully dense form of the material. Undesirably, the thermal conductivity gradually increases because the porosity gradually decreases as a consequence of sintering during high-temperature service. Because of these and other considerations such as phase transformations, the maximum allowable service temperature for yttria-partially stabilized zirconia TBCs lies in the range of about 1,200 to 1,300 °C. In contrast, the present multicomponent, rare-earth-doped, perovskite-type TBCs can withstand higher temperatures.

A material of this type comprises the following ingredients:

- The base material is a high-melting-temperature perovskite oxide — a compound having the chemical formula  $ABO_3$ , where  $A$  is a metal cation having a valence of +2 and  $B$  is a metal cation hav-

ing a valence of +4. Examples of  $A$  include Sr, Ba, Ca, and variable valence rare-earth and transition metals; examples of  $B$  include Zr and Hf.

- The base material is doped with a pair or multiple pairs of highly stable oxides of general chemical formula  $M_2O_3$ , where  $M$  is a metal cation of valence +3. The pairing of the oxides is such that they are related as electron donor and acceptor, respectively. The paired oxides can be divided into two groups, denoted I and II. Group I comprises scandia and ytterbia. The radii of their trivalent cations are smaller than those of zirconia and hafnia. The group-I cations are believed to typically become incorporated into  $B$  sites, where they are further believed to act as electron acceptors. Group II comprises neodymia, samaria, gadolinia, and lanthania. The radii of their trivalent cations are larger than that of yttria. The group-II cations are believed to typically become incorporated into  $A$  sites, where they are further believed to act as electron donors. The incorporation of the dopant trivalent cations into  $A$  and  $B$  sites enhances the stability of the base material phase and promotes the formation of significantly higher concentrations of immobile extended defects and clusters of defects, thereby greatly reducing the intrinsic thermal conductivity and the rate of sintering.
- Yttria can be included as a phase stabilizer in addition to, or instead of, the aforementioned dopant oxides.

In a preferred composition, the total concentration of yttria and/or the other

phase-stabilizing oxides lies between 4 and 30 mole percent. Ytterbia is favored over scandia as the group-I oxide because of the high cost of scandia. Alternatively, scandia in a concentration of as much as 20 percent of that of yttria can be employed to overdope the group-I oxide. Other alternative formulations are also possible.

Compositions tested to date include  $SrZrO_3$  + yttria (up to 6 mole percent) + group-I oxide (ytterbia) up to 2 mole percent + group-II oxide (gadolinia) up to 2 mole percent. Pre-sintering thermal conductivities, as determined by a laser heat-flux test at an initial surface temperature of about 3,000 °F (about 1,650 °C), have ranged between 0.6 and 0.8 W/m·K. Test data have also indicated that sintering essentially ceases after 20 hours. The thermal conductivities in the cases of compositions that include the paired doping oxides have been found to range from about a third to half of the thermal conductivities of undoped  $SrZrO_3$  and of  $SrZrO_3$  doped with yttria only. Excellent durability has also been demonstrated in the sintering and thermal-cycling tests at temperatures up to about 3,000 °F (about 1,650 °C).

*This work was done by Robert A. Miller of Glenn Research Center and Dongming Zhu of the U.S. Army Research Laboratory. Further information is contained in a TSP (see page 1).*

*Inquiries concerning rights for the commercial use of this invention should be addressed to NASA Glenn Research Center, Innovative Partnerships Office, Attn: Steve Fedor, Mail Stop 4-8, 21000 Brookpark Road, Cleveland, Ohio 44135. Refer to LEW-17432-1.*

## **Reactive Additives for Phenylethynyl-Containing Resins**

**Processability is improved.**

*Langley Research Center, Hampton, Virginia*

Phenylethynyl-containing reactive additive (PERA) compounds and mixtures have been found to be useful for improving the processability of oligomers, polymers, co-oligomers, and copolymers that

contain phenylethynyl groups. The additives can be incorporated in different forms:

- A solution of an amide acid or an imide of a PERA can be added to a

solution of phenylethynyl-containing oligomer, polymer, co-oligomer, or copolymer; or

- An imide powder of a PERA can be mixed with a dry powder of a phenyl-

ethynyl-containing oligomer, polymer, co-oligomer, or copolymer.

The effect of a given PERA on the processability and other properties of the resin system depends on whether the PERA is used in the amide acid or an imide form. With proper formulation, the PERA reduces the melt viscosity of the resin and thereby reduces the processing pressures needed to form the adhesive bonds, consolidate filled or unfilled moldings, or fabricate fiber-reinforced composite laminates. During thermal cure, a PERA reacts with itself as well as with the phenylethynyl-containing host resin and thereby becomes chemically incorporated into the resin system.

The effects of the PERA on mechanical properties, relative to those of the host resin, depend on the amount of PERA used. Typically, the incorporation of the PERA results in (1) increases in the glass-transition temperature ( $T_g$ ), modulus of elasticity, and parameters that characterize behavior under compression, and (2) greater retention of the aforementioned mechanical properties at elevated temperatures without (3) significant reduction of toughness or damage tolerance.

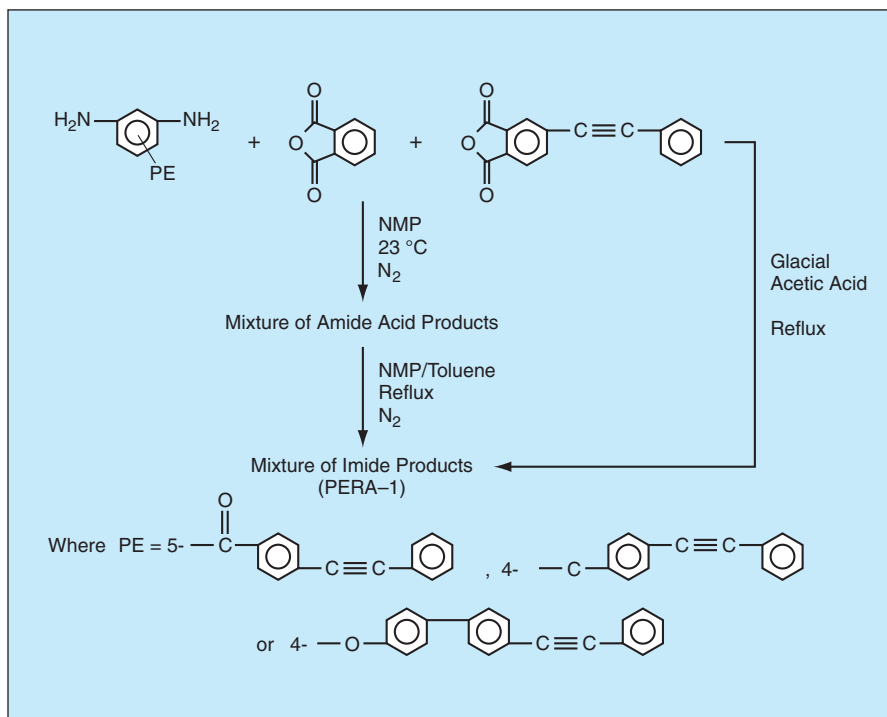
Of the formulations tested thus far, the ones found to yield the best overall results were those for which the host resin was the amide acid form of a

phenylethynyl-terminated imide (PETI) co-oligomer having a molecular weight of 5,000 g/mole [hence, designated PETI-5] and a PERA denoted as PERA-1. PETI-5 was made from 3,3',4'4'-biphenyl-tetracarboxylic dianhydride, 3,4'-oxydianiline (3,4'-ODA), 1,3-bis(3-aminophenoxy) benzene (1,3-APB), and 4-phenylethynylphthalic anhydride (PEPA). PERA-1 was made from 3,5-diamino-4'-phenylethynylbenzophenon and equimolar amounts of phthalic anhydride and PEPA. To make the imide form of PERA-1, the ingredients were reacted in glacial acetic acid. To make the amide form of PERA-1, the ingredients were reacted in N-methyl-2-pyrrolidone (NMP) under nitrogen at a temperature of 23 °C (see figure).

On the basis of the processability and other properties, a blend comprising 20 weight percent of PERA-1 and 80 weight percent PETI-5 was selected for further evaluation. Relative to neat PETI-5, the blend exhibited an increase in  $T_g$ ; improved processability; and comparable values of shear strength in adhesion to titanium panels, open-hole compressive properties, compression properties after impact, and resistance to microcracking.

*This work was done by John W. Connell, Joseph G. Smith, Jr., and Paul M. Hergenrother of Langley Research Center, and Monica L. Rommel of Northrop Grumman Corp. Further information is contained in a TSP (see page 1).*

*This invention has been patented by NASA (U.S. Patent No. 6,441,099 B1). Inquiries concerning nonexclusive or exclusive license for its commercial development should be addressed to the Patent Counsel, Langley Research Center, at (757) 864-3521. Refer to LAR-15543.*



PERA-1 is a Mixture of either amide acids or imides, depending upon which synthesis route is followed.



## Improved Gear Shapes for Face Worm Gear Drives

These shapes offer potential for increasing precision and reducing vibration and noise.

*John H. Glenn Research Center, Cleveland, Ohio*

Shapes different from the traditional ones have been proposed for face worm gears and for conical and cylindrical worms that mesh with them. The proposed shapes are based on the concept of generating a face worm gear surface by use of a tilted head cutter instead of the traditional use of a hob. (As used

here, “head cutter” is also meant to signify, alternatively, a head grinding tool.) The gear-surface-generation equipment would be similar to that used for generation of spiral bevel and hypoid gears. In comparison with the corresponding traditional hob, a tilted head cutter according to the proposal would be larger,

could be fabricated with greater precision, and would enable the generation of gear surfaces with greater precision and greater productivity.

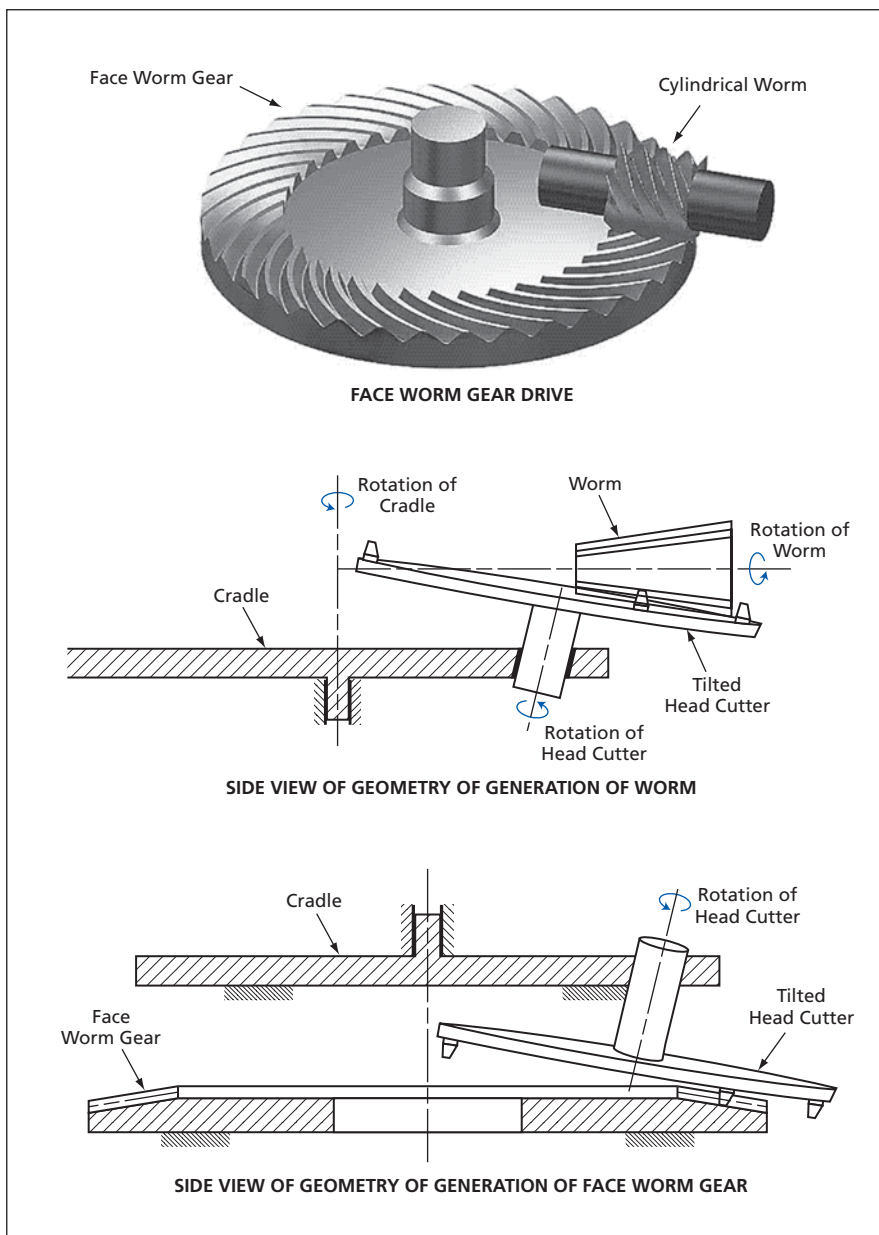
A face worm gear would be generated (see figure) by use of a tilted head cutter, the blades or grinding surfaces of which would have straight-line profiles. The tilt of the head cutter would prevent interference with teeth adjacent to the groove being cut or ground.

A worm to mesh with the face worm gear would be generated by use of a tilted head cutter mounted on the cradle of a generating machine. The blades or grinding surfaces of the head cutter would have a parabolic profile and would deviate from the straight-line profiles of the head cutter for the face worm gear. The shortest distance between the worm and the cradle would follow a parabolic function during the cycle of meshing in the generating process to provide a parabolic function of transmission errors to the gear drive.

The small mismatch between the profiles of the face-worm-gear and worm head cutters would make it possible to localize the bearing contact in the worm gear drive. The parabolic function of transmission errors could absorb discontinuous linear functions of transmission errors caused by errors of alignment; this could afford a significant benefit, in that such errors are main sources of noise and vibration in gear drives.

The main advantage of using tilted head cutters is that cutting speeds are independent of the shape-generation processes, making it possible to choose cutting speeds that are optimum with respect to requirements to minimize temperatures and deformations during fabrication and improve the quality of finished parts.

The profile of the cutting or grinding surface and the machine-tool settings for the position and orientation of a head cutter would be derived from the theoretical shape generated by a hob. The derivation would be effected by use of an algorithm that takes account of the tilted-head-cutter geometry and enforces



A Face Worm Gear and a Cylindrical Worm that meshes with it would be fabricated by use of tilted head cutters.

the requirements for meshing and non-interference.

A tooth-contact-analysis computer program has been developed for simulation of meshing and contact of the proposed worms and face worm gears. In a test case, the program showed that, as desired, the function of transmission errors would be a parabolic function of low magnitude, the contact would be localized, and the path of contact would

be longitudinal in the sense that it would lie along the gear-tooth surfaces. The program also showed that the bearing contact region would be free of areas of severe contact stresses and that the contact ratio would be larger than 3 (signifying that at any given instant, there would be at least 3 pairs of teeth in contact).

*This work was done by Faydor L. Litvin, Alessandro Nava, Qi Fan, and Alfonso*

*Fuentes of the University of Illinois for Glenn Research Center. Further information is contained in a TSP (see page 1).*

*Inquiries concerning rights for the commercial use of this invention should be addressed to NASA Glenn Research Center, Innovative Partnerships Office, Attn: Steve Fedor, Mail Stop 4-8, 21000 Brookpark Road, Cleveland, Ohio 44135. Refer to LEW-17596-1.*

## Alternative Way of Shifting Mass To Move a Spherical Robot

**A payload would change its position by lengthening and shortening suspension cables.**

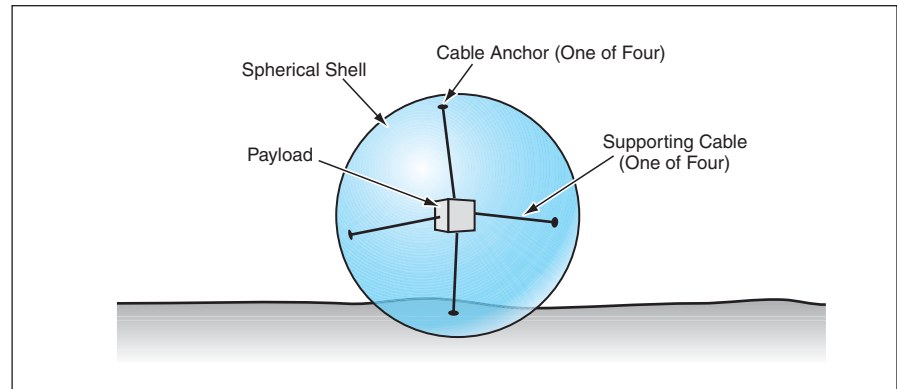
*NASA's Jet Propulsion Laboratory, Pasadena, California*

An alternative method of controlled shifting of the center of mass has been proposed as a means of locomotion of a robot that comprises mostly a payload inside a hollow, approximately spherical shell. The method would be applicable to robots that include rigid, semirigid, or flexible inflated shells, including those of the "beach-ball rover" type, variants of which have been described in several previous *NASA Tech Briefs* articles.

A prior method, to which the method now proposed would be an alternative, was described in "'Beach-Ball' Robotic Rovers" (NPO-19272), *NASA Tech Briefs*, Vol. 19, No. 11 (November 1995), page 83. To recapitulate: Three diametral tethers approximately perpendicular to each other would be attached to the shell, effectively defining an approximate Cartesian coordinate system within the shell. A control box containing motors and power and control circuits would move itself along the tethers and adjust the lengths of the tethers in a coordinated fashion to shift the center of gravity and thereby cause the shell to roll in a desired direction.

The method now proposed calls for suspending a payload by use of four or more cables that would be anchored to the inner surface of the sphere. In this method, the anchor points would not be diametrically opposite points defining Cartesian axes. The payload, which includes the functional analog of the aforementioned control box, would contain winches that would shorten or lengthen the cables in a coordinated manner to shift the position of the payload within the shell.

In a typical case, the locomotion system would include four cables an-



The Payload Would Contain Winches that would extend some cables while retracting others to move itself to a specified position within the spherical shell.

chored at approximately the corners of a regular tetrahedron (see figure). Optionally, one could use more than four cables for redundancy against potential failure and/or as a means of distributing the weight of the payload to multiple anchor points to reduce localized stress on the spherical shell. The arrangement of anchor points would not be critical as long as they defined at least three different axes of motion in at least two different planes; hence, the proposed method would afford robustness of motion control in the face of deformation of the spherical shell.

Simple wires could be used to connect the payload to any sensors mounted on the outer or inner surface of the shell. The wires would have to be long enough to reach the maximum distance, and would have to hang slack when the distance was less. Because there would be little rotation between the payload and the spherical shell, it is unlikely that the wires would become tangled; however, one might wish to include spring-loaded

retractors to minimize the probability of entanglement.

In the case of a flexible shell, all the cables supporting the payload could be retracted or extended to some extent to increase or decrease, respectively, the pressure of gas inside the shell. Another option would be to include spring-loaded supporting cables not connected to winches, in addition to those that were connected to winches; this option may make it possible to reduce the number of winches while obtaining an adequate range of motion.

Yet another option would be to use rigid rods and linear actuators instead of cables and winches. However, rods and linear actuators would probably weigh more than would cables and winches. Moreover, this option would not be compatible with a flexible shell.

*This work was done by James Lux of Caltech for NASA's Jet Propulsion Laboratory. Further information is contained in a TSP (see page 1). NPO-30491*

## Parylene C as a Sacrificial Material for Microfabrication

*Goddard Space Flight Center, Greenbelt, Maryland*

Parylene C has been investigated for use as a sacrificial material in microfabrication. Although Parylene C cannot be patterned lithographically like photoresists, it nevertheless extends the range of processing options by offering a set of properties that are suitable for microfabrication and are complementary to those of photoresists. The compatibility of Parylene C with several microfabrication processes was demonstrated in experiments in which a thin film of Parylene C was deposited on a silicon wafer, then several thin metal films were deposited and successfully patterned, utilizing the Parylene C pads as a sacrificial layer.

The term “parylene” — a contraction of “poly(para-xylene)” — denotes a family of vapor-deposited polymers. In Parylene C (the most common form of parylene), a chlorine atom is substituted for one of the hydrogen atoms on the benzene ring of each para-xylene moiety. Heretofore, parylenes have been used as conformal coating materials in diverse applications.

The unique combinations of processing properties of Parylene C that make it suitable for use in microfabrication are the following:

- It can be deposited to uniform sub-micron thickness.
- It is highly resistant to solvents and, therefore, able to survive wet processing.
- It can easily be patterned or removed by use of oxygen plasma.
- Because it cannot be easily patterned or removed by means other than oxygen plasma, it can withstand many dry etching processes.
- It has little or no outgassing and is fully functional at cryogenic temperatures.

*This work was done by Michael Beamesderfer of Goddard Space Flight Center.*

*This invention is owned by NASA, and a patent application has been filed. Inquiries concerning nonexclusive or exclusive license for its commercial development should be addressed to the Patent Counsel, Goddard Space Flight Center, (301) 286-7351. Refer to GSC-14803-1.*

## In Situ Electrochemical Deposition of Microscopic Wires

**Tedious, expensive post-growth assembly is no longer necessary.**

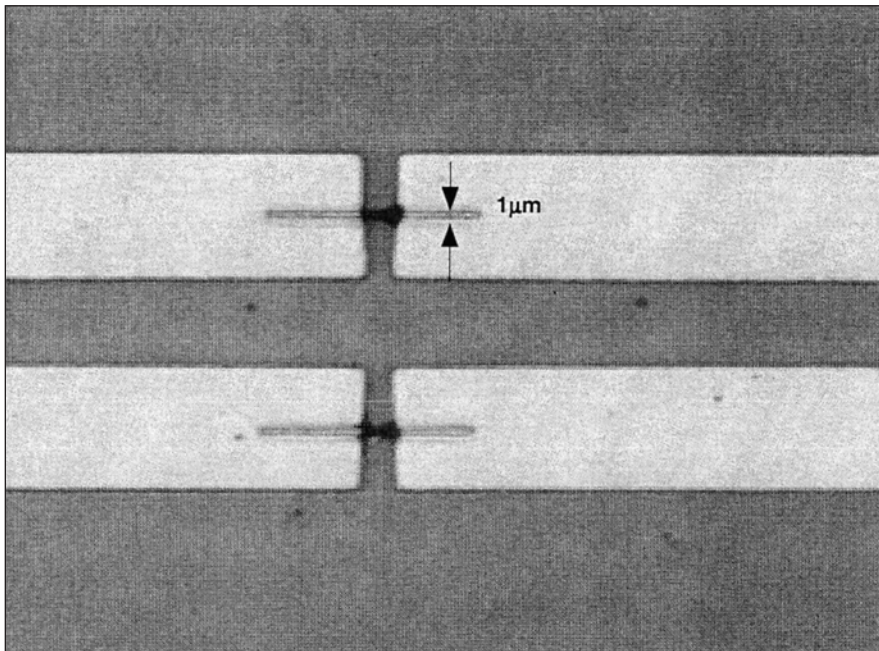
*NASA's Jet Propulsion Laboratory, Pasadena, California*

A method of fabrication of wires having micron and submicron dimensions is built around electrochemical deposition of the wires in their final positions be-

tween electrodes in integrated circuits or other devices in which the wires are to be used. Heretofore, nanowires have been fabricated by a variety of techniques char-

acterized by low degrees of controllability and low throughput rates, and it has been necessary to align and electrically connect the wires in their final positions by use of sophisticated equipment in expensive and tedious post-growth assembly processes. The present method is more economical, offers higher yields, enables control of wire widths, and eliminates the need for post-growth assembly. The wires fabricated by this method could be used as simple electrical conductors or as transducers in sensors. Depending upon electrodeposition conditions and the compositions of the electroplating solutions in specific applications, the wires could be made of metals, alloys, metal oxides, semiconductors, or electrically conductive polymers.

In this method, one uses fabrication processes that are standard in the semiconductor industry. These include cleaning, dry etching, low-pressure chemical vapor deposition, lithography, dielectric deposition, electron-beam lithography, and metallization processes as well as the electrochemical deposition process used to form the wires. In a typical case of fabrication of a circuit that includes electrodes between which microscopic wires are to be formed on a silicon substrate,



**Palladium Wires** 1  $\mu\text{m}$  wide and 5  $\mu\text{m}$  long were formed in contact with gold electrodes by electrodeposition into 1- $\mu\text{m}$ -wide channels from a solution of  $\text{Pd}(\text{NH}_3)_2(\text{NO}_3)_2$  at a concentration of 10 g/L and ammonium sulfate at a concentration of 100 g/L.

the fabrication processes follow a standard sequence until just before the fabrication of the microscopic wires.

Then, by use of a thermal SiO<sub>2</sub>-deposition technique, the electrodes and the substrate surface areas in the gaps between them are covered with SiO<sub>2</sub>. Next, the SiO<sub>2</sub> is electron-beam patterned, then reactive-ion etched to form channels having specified widths (typically about 1 μm or less) that define the widths of the wires to be formed. Drops of an electroplating solution are placed on the substrate in the regions containing the channels thus

formed, then the wires are electrodeposited from the solution onto the exposed portions of the electrodes and into the channels. The electrodeposition is a room-temperature, atmospheric-pressure process. The figure shows an example of palladium wires that were electrodeposited into 1-mm-wide channels between gold electrodes.

*This work was done by Minhee Yun, Nosang Myung, and Richard Vasquez of Caltech for NASA's Jet Propulsion Laboratory. Further information is contained in a TSP (see page 1).*

*In accordance with Public Law 96-517, the contractor has elected to retain title to this invention. Inquiries concerning rights for its commercial use should be addressed to:*

*Innovative Technology Assets Management  
JPL*

*Mail Stop 202-233  
4800 Oak Grove Drive  
Pasadena, CA 91109-8099  
(818) 354-2240*

*E-mail: iaoffice@jpl.nasa.gov*

*Refer to NPO-40221, volume and number of this NASA Tech Briefs issue, and the page number.*

## Improved Method of Manufacturing SiC Devices

Several improvements promise to make manufacture of SiC devices more economical.

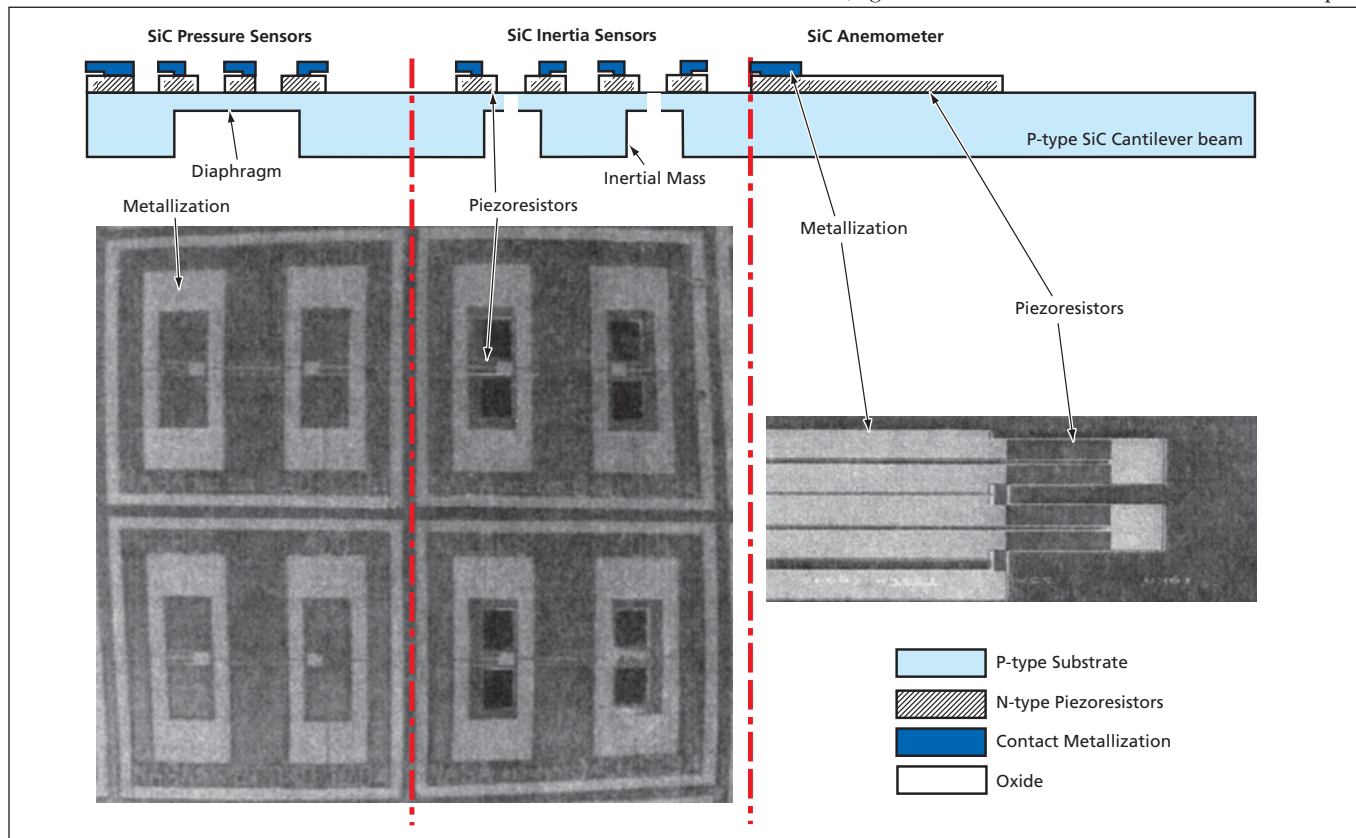
*John H. Glenn Research Center, Cleveland, Ohio*

The phrase, “common-layered architecture for semiconductor silicon carbide” (“CLASSiC”) denotes a method of batch fabrication of microelectromechanical and semiconductor devices from bulk silicon carbide. CLASSiC is the latest in a series of related methods developed in recent years in continuing efforts to standardize SiC-fabrication

processes. CLASSiC encompasses both institutional and technological innovations that can be exploited separately or in combination to make the manufacture of SiC devices more economical. Examples of such devices are piezoresistive pressure sensors, strain gauges, vibration sensors, and turbulence-intensity sensors for use in harsh environments (e.g.,

high-temperature, high-pressure, corrosive atmospheres).

The institutional innovation is to manufacture devices for different customers (individuals, companies, and/or other entities) simultaneously in the same batch. This innovation is based on utilization of the capability for fabrication, on the same substrate, of multiple



Two Pressure Sensors, Two Accelerometers, and an Anemometer were fabricated on the same SiC substrate to demonstrate the capability for simultaneous batch fabrication of devices that perform different functions. Cross-sectional views of devices are also shown.

SiC devices having different functionalities (see figure). Multiple customers can purchase shares of the area on the same substrate, each customer's share being apportioned according to the customer's production-volume requirement. This makes it possible for multiple customers to share costs in a common foundry, so that the capital equipment cost per customer in the inherently low-volume SiC-product market can be reduced significantly.

One of the technological innovations is a five-mask process that is based on an established set of process design rules. The rules provide for standardization of the fabrication process, yet are flexible enough to enable multiple customers to lay out masks for their portions of the SiC substrate to provide for simultaneous batch fabrication of their various devices. In a related prior method, denoted multi-user fabrication in silicon carbide (MUSiC), the fabrication process is based largely on surface micromachining of poly SiC. However, in MUSiC one cannot exploit the superior sensing, thermomechanical, and elec-

trical properties of single-crystal 6H-SiC or 4H-SiC. As a complement to MUSiC, the CLASSiC five-mask process can be utilized to fabricate multiple devices in bulk single-crystal SiC of any polytype. The five-mask process makes fabrication less complex because it eliminates the need for large-area deposition and removal of sacrificial material.

Other innovations in CLASSiC pertain to selective etching of indium tin oxide and aluminum in connection with multilayer metallization. One major characteristic of bulk micromachined microelectromechanical devices is the presence of three-dimensional (3D) structures. Any 3D recesses that already exist at a given step in a fabrication process usually make it difficult to apply a planar coat of photoresist for metallization and other subsequent process steps. To overcome this difficulty, the CLASSiC process includes a reversal of part of the conventional flow: Metallization is performed before the recesses are etched.

The metallization is followed by the deposition and lift-off of aluminum

and indium tin oxide etch masks on the entire planar SiC substrate surface except where the recesses are to be created. After etching of the recesses, the aluminum and indium tin oxide etch masks are selectively etched to leave a stack of underlying metals (example, titanium, tantalum silicide, and platinum). Thus, the aluminum and indium tin oxide serve as protective layers for the metallization while also functioning as etch masks during deep reactive-ion etching to create the desired 3D structures. After removal of the aluminum and indium tin oxide, wires can be bonded onto the top platinum layer to provide for transition of electrical signals to/from the device.

*This work was done by Robert S. Okojie of Glenn Research Center. Further information is contained in a TSP (see page 1).*

*Inquiries concerning rights for the commercial use of this invention should be addressed to NASA Glenn Research Center, Innovative Partnerships Office, Attn: Steve Fedor, Mail Stop 4-8, 21000 Brookpark Road, Cleveland, Ohio 44135. Refer to LEW-17170.*





## Microwave Treatment of Prostate Cancer and Hyperplasia

**Additional uses are found for a relatively inexpensive microwave treatment system.**

*Lyndon B. Johnson Space Center, Houston, Texas*

Microwave ablation in the form of microwave energy applied to a heart muscle by a coaxial catheter inserted in a vein in the groin area can be used to heat and kill diseased heart cells. A microwave catheter has been developed to provide deep myocardial ablation to treat ventricular tachycardia by restoring appropriate electrical activity within the heart and eliminating irregular heartbeats. The resulting microwave catheter design, which is now being developed for commercial use in treating ventricular tachycardia, can be modified to treat prostate cancer and benign prostatic hyperplasia (BPH). Inasmuch as the occurrence of BPH is increasing — currently 350,000 operations per year are performed in the United States alone to treat this condition — this microwave catheter has significant commercial potential.

The microwave operating frequency affects the heating depth. An electrophysiologist will be able to take advantage of the physics of depth of penetration (in particular, the variations of conductivity and permittivity of tissue with frequency) to focus the microwave beam. The power level and delivery time also affect the balance between the increase in heat (due to the absorption of microwave energy) and the loss of heat (due to conduction away from targeted cells). A computer program that simulates the heating profile has been written to assist in determining the balance needed to necrose targeted cells while saving non-targeted cells.

There are several variations of microwave radiators suitable for treating specific regions of the prostate or the prostate as a whole. The following three configurations are suitable for treating specific conditions and specific locations:

- *Single Antenna Within the Urethra*

A single antenna radiates within the urethra. A urethra catheter can be made to include a phase-change material surrounding the radiation tip to prevent a significant temperature rise without need for a water cooling system. The phase-change material must, of course, be nearly transparent to the microwave radiation. This material provides localized cooling to protect the urethra from damage, but permits microwave heating to occur beyond the urethra, into the prostate. For treatment over the entire prostate, or over large regions of the prostate, it may be necessary to use several throwaway catheters because one may not contain sufficient phase-change material. Calculations have shown the feasibility of this approach, provided that a phase-change material that has the desired characteristics can be found.

- *Multiple Colon Antennas*

Multiple colon catheter antennas can be phased and directed toward the prostate to provide localized temperature gradients in the regions of the prostate located near the colon. Cooling must be provided to protect the colon and the intervening tissue. Prostate cancer often begins in the prostate near the colon and should be treatable with this

technique. Computer simulations show that by adjusting the locations of the microwave radiators and the phases of their microwave signals, the heating centers in the prostate can be adjusted to necrose critical regions only.

- *Single Urethra Antenna and Two Colon Antennas*

Combinations of urethra and colon microwave radiators can be used to provide treatment appropriate to specific problems. Generally, one microwave catheter in the urethra, when working together with one or more catheters in the colon, can provide localized heating to satisfy most requirements. By adjustment of frequency, phase, directionality, and duration of the microwave radiation, one can select from among a wide array of heating profiles in the prostate. Computer simulations indicate that these three antennas can be properly phased together for focusing the heated region.

Laboratory tests of the single urethra antenna and two colon antennas are now underway, using phantom material to represent the prostate gland.

*This work was done by G. Dickey Arndt and Phong Ngo of Johnson Space Center, J. R. Carl of Advanced Electromagnetics, and George Raffoul, consultant.*

*This invention is owned by NASA, and a patent application has been filed. Inquiries concerning nonexclusive or exclusive license for its commercial development should be addressed to the Patent Counsel, Johnson Space Center, (281) 483-0837. Refer to MSC-23049.*





## Ferroelectric Devices Emit Charged Particles and Radiation

Compact, lightweight, low-power sources could be useful in numerous applications.

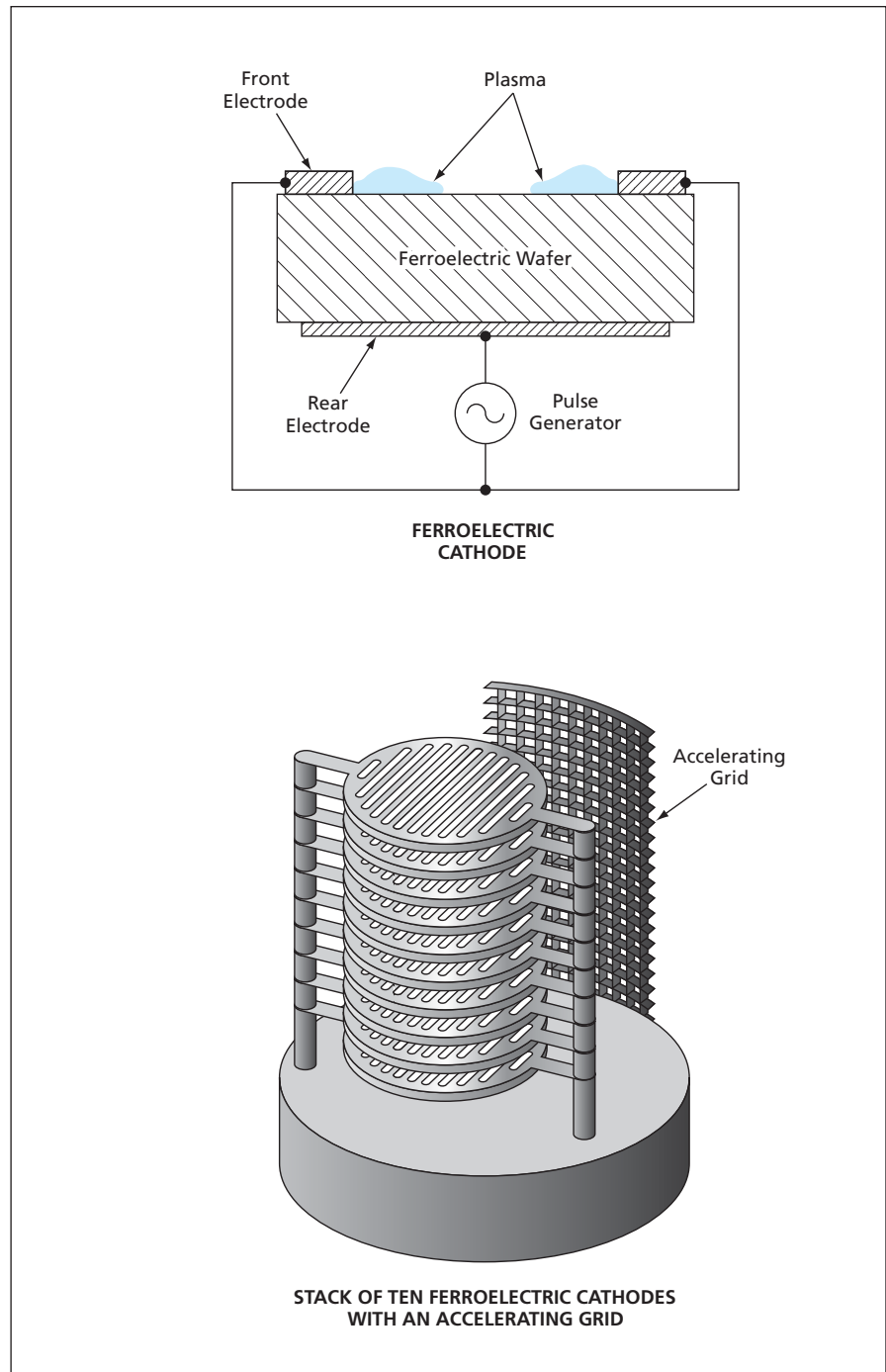
NASA's Jet Propulsion Laboratory, Pasadena, California

Devices called “solid-state ferroelectric-based sources” (SSFBSs) are under development as sources of electrons, ions, ultraviolet light, and x-rays for diverse applications in characterization and processing of materials. Whereas heretofore it has been necessary to use a different device to generate each of the aforementioned species of charged particles or radiation, a single SSFBS can be configured and operated to selectively generate any of the species as needed using a single source. Relative to comparable prior sources based, variously, on field emission, thermionic emission, and gaseous discharge plasmas, SSFBSs demand less power, and are compact and lightweight.

An SSFBS exploits the unique physical characteristics of a ferroelectric material in the presence of a high-frequency pulsed electric field. The basic building block of an SSFBS is a ferroelectric cathode — a ferroelectric wafer with a solid electrode covering its rear face and a grid electrode on its front face (see figure). The application of a voltage pulse — typically having amplitude of several kilovolts and duration of several nanoseconds — causes dense surface plasma to form near the grid wires on the front surface.

The shape of the applied voltage waveform determines the characteristics of the emitted charged particles and radiation and can be tailored to maximize the yield of electrons or ions. For example, one could utilize bipolar pulsing and/or a succession of pulses with different time intervals between them. Although the parameters of the surface plasma do not depend strongly on the polarity of the voltage, it is preferable to apply negative pulses to the rear (solid) electrode while keeping the front (grid) electrode at ground potential.

The plasma generates intense visible and ultraviolet light. If a grid is placed at a suitable short distance near the front face and a synchronized positive voltage pulse is applied to this grid, then electrons are extracted from the plasma and accelerated toward and through the



A **Ferroelectric Cathode** is the basic building block of an SSFBS. To enhance performance, one could construct an SSFBS containing an array of multiple ferroelectric cathodes electrically connected in parallel, possibly in combination with one or more accelerating grid(s). The array and/or the grid(s) could have any of a large variety of shapes.

grid. The resulting electron beam can be aimed at a target. The impingement of the energetic electrons on a suitable target can be utilized to generate x-rays. Another option is to pulse an accelerating grid negative with respect to the front face so as to extract and accelerate positive ions.

Typical parameters of an optimized design for a basic SSFB include a ferroelectric-plasma area of  $10 \text{ cm}^2$ , operating pressure of about  $10^{-2}$  torr (about 1.3 Pa), pulse-repetition frequency of 20 Hz, electron or ion current up to 10 A under an accelerating pulse of 30-kV amplitude and 50-ns duration.

*This work was done by Yoseph Bar-Cohen, Stewart Sherrit, Xiaoqi Bao, Joshua Felsteiner, and Yakov Karsik of Caltech for NASA's Jet Propulsion Laboratory. Further information is contained in a TSP (see page 1). NPO-30694*

## Dusty-Plasma Particle Accelerator

**Microparticles and nanoparticles can be accelerated to controllable kinetic energies.**

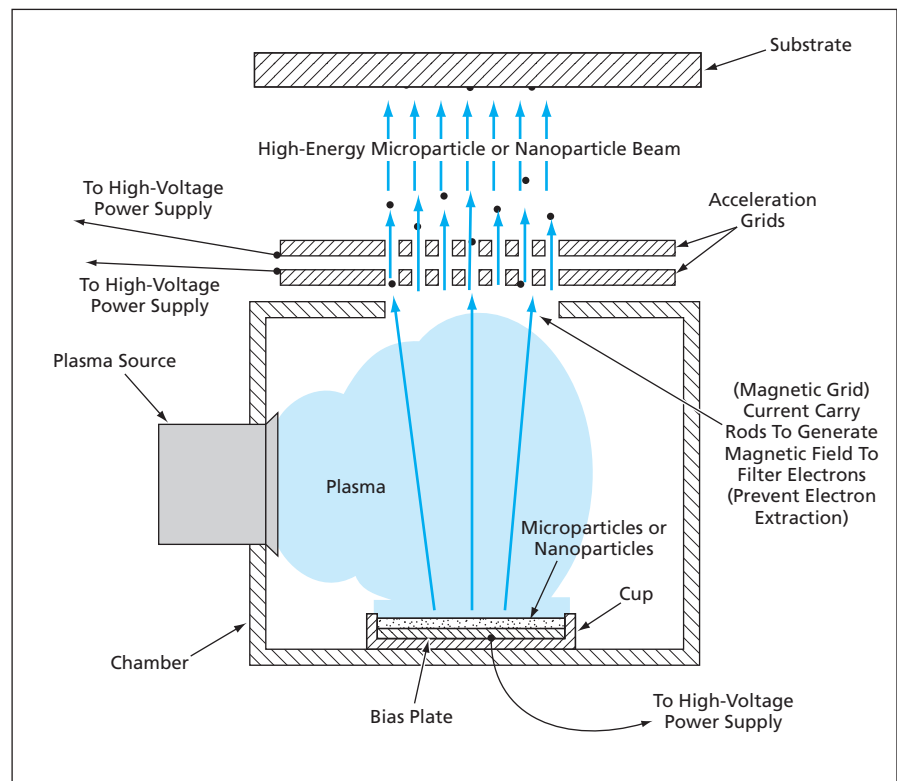
*John H. Glenn Research Center, Cleveland, Ohio*

A dusty-plasma apparatus is being investigated as means of accelerating nanometer- and micrometer-sized particles. Applications for the dusty-plasma particle accelerators fall into two classes:

- Simulation of a variety of rapidly moving dust particles and micrometeoroids in outer-space environments that include micrometeoroid streams, comet tails, planetary rings, and nebulae and
- Deposition or implantation of nanoparticles on substrates for diverse industrial purposes that could include hardening, increasing thermal insulation, altering optical properties, and/or increasing permittivities of substrate materials.

Relative to prior apparatuses used for similar applications, dusty-plasma particle accelerators offer such potential advantages as smaller size, lower cost, less complexity, and increased particle flux densities.

A dusty-plasma particle accelerator exploits the fact that an isolated particle immersed in plasma acquires a net electric charge that depends on the relative mobilities of electrons and ions. Typically, a particle that is immersed in a low-temperature, partially ionized gas, wherein the average kinetic energy of electrons exceeds that of ions, causes the particle to become negatively charged. The particle can then be accelerated by applying an appropriate electric field. A dusty-plasma particle accelerator (see figure) includes a plasma source such as a radio-frequency induction discharge apparatus containing (1) a shallow cup with a biasable electrode to hold the particles to be accelerated and (2) a holder for the substrate on which the particles are to impinge. Depending on the specific design, a pair of electrostatic-acceleration grids between the substrate and discharge plasma can be used to both collimate and further



In a **Dusty-Plasma Particle Accelerator**, microparticles or nanoparticles in a cup exposed to a plasma become electrically charged and are then accelerated by applying a pulsed electric field.

accelerate particles exiting the particle holder. Once exposed to the discharge plasma, the particles in the cup quickly acquire a negative charge. Application of a negative voltage pulse to the biasable electrode results in the initiation of a low-current, high-voltage cathode spot. Plasma pressure associated with the cathode spot as well as the large voltage drop at the cathode spot accelerates the charged particles toward the substrate. The ultimate kinetic energy attained by particles exiting the particle holder depends in part on the magnitude of the cathode spot sheath potential difference, which is proportional to

the magnitude of the voltage pulse, and the on the electric charge on the dust. The magnitude of the voltage pulse can be controlled directly, whereas the particle's electric charge can be controlled indirectly by controlling the operating parameters of the plasma apparatus.

*This work was done by John E. Foster of Glenn Research Center. Further information is contained in a TSP (see page 1).*

*Inquiries concerning rights for the commercial use of this invention should be addressed to NASA Glenn Research Center, Innovative Partnerships Office, Attn: Steve Fedor, Mail Stop 4-8, 21000 Brookpark Road, Cleveland, Ohio 44135. Refer to LEW-17438.*

# Frozen-Plug Technique for Liquid-Oxygen Plumbing

An established plumbing technique is extended to systems other than water pipes.

*John F. Kennedy Space Center, Florida*

A frozen-plug technique has been conceived as a means of temporarily blocking the flow of liquid oxygen or its vapor through a tube or pipe. The technique makes it possible to perform maintenance, repair, or other work on downstream parts of the cryogenic system in which the oxygen is used, without having to empty an upstream liquid-oxygen reservoir and, hence, without wasting the stored liquid oxygen and without subjecting the reservoir to the stresses of thermal cycling.

The present frozen-plug technique was inspired by an older frozen-plug technique used by plumbers on water pipes in situations in which the expansion of water ice can be tolerated. In a typical application of the older technique, the affected section of pipe is cooled by use of carbon dioxide or liquid nitrogen, causing the water in the affected section of pipe to freeze.

In the present frozen-plug technique, the section of pipe to be plugged is wrapped with a tube or vessel that can be filled with a suitable cryogen. A sec-

ondary fluid that is compatible with oxygen and that has a freezing temperature higher than that of oxygen is pumped into the pipe under pressure, completely filling the affected section. The higher freezing temperature of the secondary fluid makes it easier and safer to use the secondary fluid than to fill the pipe with liquid oxygen. In the initial application for which the technique was conceived, an oxygen-compatible cleaning solvent was chosen as secondary fluid because of an application-specific requirement to maintain cleanliness in the cryogenic system. Other secondary fluids may be suitable in other applications.

The cryogen is pumped into the tube or vessel wrapped around the pipe. The cryogen (typically, liquid nitrogen) is chosen to have a temperature lower than the freezing temperature of the secondary fluid. Therefore, the pipe and its contents become chilled below the freezing temperature of the secondary fluid, so that a plug of frozen secondary fluid forms in the pipe. The

plug can withstand the upstream and downstream pressures and the differential pressure between them.

The present frozen-plug technique is adaptable to systems containing fluids other than the liquid oxygen of its original application, and to the use of secondary fluids that are not cleaning solvents. Moreover, the choice of cryogen in this technique is not limited to liquid nitrogen. The technique can also be adapted to non-cryogenic systems. In systems in which freezing of the commodity fluids (perhaps some food products, for example) can be tolerated, there may be no need to use secondary fluids. In cases of some commodities, it may be necessary to perform research to identify any potential hazards posed by freezing.

*This work was done by C. E. "Mac" McCaskey of Kennedy Space Center and Dennis Lobmeyer, Zoltan Nagy, and Rich Peltzer of Dynacs, Inc. For further information, contact the Kennedy Innovative Partnerships Office at (321) 867-8130.  
KSC-12382*





## Books & Reports

### Shock Waves in a Bose-Einstein Condensate

A paper presents a theoretical study of shock waves in a trapped Bose-Einstein condensate (BEC). The mathematical model of the BEC in this study is a nonlinear Schrödinger equation (NLSE) in which (1) the role of the wave function of a single particle in the traditional Schrödinger equation is played by a space- and time-dependent complex order parameter  $\psi(\mathbf{x}, t)$  proportional to the square root of the density of atoms and (2) the atoms engage in a repulsive interaction characterized by a potential proportional to  $|\psi(\mathbf{x}, t)|^2$ . Equations that describe macroscopic perturbations of the BEC at zero temperature are derived from the NLSE and simplifying assumptions are made, leading to equations for the propagation of sound waves and the transformation of sound waves into shock waves. Equations for the speeds of shock waves and the relationships between jumps of velocity and density across shock fronts are derived. Similarities and differences between this theory and the classical theory of sound waves and shocks in ordinary gases are noted. The present theory is illustrated by solving the equations for the example of a shock wave propagating in a cigar-shaped BEC.

*This work was done by Igor Kulikov and Michail Zak of Caltech for NASA's Jet Propulsion Laboratory. Further information is contained in a TSP (see page 1). NPO-30593*

### Progress on a Multichannel, Dual-Mixer Stability Analyzer

Several documents describe aspects of the continuing development of a multichannel, dual-mixer system for simultaneous characterization of the instabilities of multiple precise, low-noise oscillators. One of the documents presents the basic principles and design concept that were summarized in "Oscillator-Stability Analyzer Based on a Time-Tag Counter" (NPO-20749), *NASA Tech Briefs*, Vol. 25, No. 5 (May 2001), page 48. To recapitulate: One of the oscillators would be deemed to be a reference oscillator, its frequency would be offset by an amount (100 Hz) much greater than the desired data rate, and

each of the other oscillators would be compared with the frequency-offset signal by operation of a combination of hardware and software. A high-rate time-tag counter would collect zero-crossing times of the  $\approx 100$ -Hz beat notes. The system would effect a combination of interpolation and averaging to process the time tags into low-rate phase residuals at the desired grid times. Circuitry that has been developed since the cited prior article includes an eight-channel timer board to replace an obsolete commercial time-tag counter, plus a custom offset generator, cleanup loop, distribution amplifier, zero-crossing detector, and frequency divider.

*This work was done by Albert Kirk, Steven Cole, Gary Stevens, Blake Tucker, and Charles Greenhall of Caltech for NASA's Jet Propulsion Laboratory. Further information is contained in a TSP (see page 1). NPO-40468*

### Development of Carbon-Nanotube/Polymer Composites

A report presents a short discussion of one company's effort to develop composites of carbon nanotubes in epoxy and other polymer matrices. The focus of the discussion is on the desirability of chemically modifying carbon nanotubes to overcome their inherent chemical nonreactivity and thereby enable the formation of strong chemical bonds between nanotubes and epoxies (or other polymeric matrix materials or their monomeric precursors). The chemical modification is effected in a process in which discrete functional groups are covalently attached to the nanotube surfaces. The functionalization process was proposed by the company and demonstrated in practice for the first time during this development effort. The covalently attached functional groups are capable of reacting with the epoxy or other matrix resin to form covalent bonds. Furthermore, the company uses this process to chemically modify the nanotube surfaces, affording "tunable" adhesion to polymers and solubility in select solvents. Flat-sheet composites containing functionalized nanotubes demonstrate significantly improved mechanical, thermal, and electrical properties.

*This work was done by Thomas A. Reynolds of ReyTech Corp. for Johnson*

*Space Center. For further information, contact the Johnson Innovative Partnerships Office at (281) 483-3809. MSC-23428*

### Thermal Imaging of Earth for Accurate Pointing of Deep-Space Antennas

A report discusses a proposal to use thermal (long-wavelength infrared) images of the Earth, as seen from spacecraft at interplanetary distances, for pointing antennas and telescopes toward the Earth for Ka-band and optical communications. The purpose is to overcome two limitations of using visible images: (1) at large Earth phase angles, the light from the Earth is too faint; and (2) performance is degraded by large albedo variations associated with weather changes. In particular, it is proposed to use images in the wavelength band of 8 to 13  $\mu\text{m}$ , wherein the appearance of the Earth is substantially independent of the Earth phase angle and emissivity variations are small. The report addresses tracking requirements for optical and Ka-band communications, selection of the wavelength band, available signal level versus phase angle, background noise, and signal-to-noise ratio. Tracking errors are estimated for several conceptual systems employing currently available infrared image sensors. It is found that at Mars range, it should be possible to locate the centroid of the Earth image within a noise equivalent angle (a random angular error) between 10 and 150 nanoradians at a bias error of no more than 80 nanoradians.

*This work was done by Gerardo Ortiz and Shinhak Lee of Caltech for NASA's Jet Propulsion Laboratory. Further information is contained in a TSP (see page 1). NPO-40395*

### Modifications of a Composite-Material Combustion Chamber

Two short reports discuss modifications of a small, lightweight combustion chamber that comprises a carbon/carbon composite outer shell and an iridium/rhenium inner liner. The first report discusses chamber design modifications made as results of hot-fire tests and post-test characterization. The

modifications were intended to serve a variety of purposes, including improving fabrication, reducing thermal-expansion mismatch stresses, increasing strength-to-weight ratios of some components, and improving cooling of some components. The second report discusses (1) the origin of stress in the mismatch between the thermal expansions of the Ir/Re liner and a niobium sleeve and flange attached to the carbon/carbon shell and (2) a modification intended to relieve the stress. The modification involves the redesign of an inlet connection to incorporate a compressible seal between the Ir/Re liner and the Nb flange. A nickel alloy was selected as the seal material on the basis of its thermal-expansion properties and its ability to withstand the anticipated stresses, including the greatest stresses caused by the high temperatures to be used in brazing during fabrication.

*This work was done by Brian E. Williams and Shawn R. McNeal of Ultramet for Johnson Space Center. For further information, contact the Johnson Innovative Partnerships Office at (281) 483-3809. MSC-22981/82*



### Modeling and Diagnostic Software for Liquefying-Fuel Rockets

A report presents a study of five modeling and diagnostic computer programs considered for use in an integrated vehicle health management (IVHM) system during testing of liquefying-fuel hybrid rocket engines in the Hybrid Combustion

Facility (HCF) at NASA Ames Research Center. Three of the programs — TEAMS, L2, and RODON — are model-based reasoning (or diagnostic) programs. The other two programs — ICS and IMS — do not attempt to isolate the causes of failures but can be used for detecting faults. In the study, qualitative models (in TEAMS and L2) and quantitative models (in RODON) having varying scope and completeness were created. Each of the models captured the structure and behavior of the HCF as a physical system. It was noted that in the cases of the qualitative models, the temporal aspects of the behavior of the HCF and the abstraction of sensor data are handled outside of the models, and it is necessary to develop additional code for this purpose. A need for additional code was also noted in the case of the quantitative model, though the amount of development effort needed was found to be less than that for the qualitative models.

*This work was done by Scott Poll, David Iverson, Jeremy Ou, Dwight Sanderfer, and Ann Patterson-Hine of Ames Research Center. Further information is contained in a TSP (see page 1).*

*Inquiries concerning rights for the commercial use of this invention should be addressed to the Innovative Partnerships Division, Ames Research Center, (650) 604-2954. Refer to ARC-15341-1.*



### Spacecraft Antenna Clusters for High EIRP

Several documents in a collection discuss a proposal to use clusters of appro-

priately phased, relatively small microwave antennas to obtain high levels of effective isotropically radiated power (EIRP) for transmission of data from spacecraft to Earth during exploration of distant planets. The advantages of such a cluster, relative to a single larger antenna of equivalent EIRP, would include the following:

- The cluster would have less mass and volume.
- Power densities in amplifiers, waveguides, and other transmitting components feeding the antennas would be lower. Therefore, problems of preventing overheating and high-voltage breakdown would be less severe.
- Phases could be made electronically adjustable for beam steering to increase pointing accuracy.
- Failure of one antenna or its feed system would reduce the EIRP but would not disable the entire transmitting system. Beam-steering capability would remain as long as at least three antennas (and their feed systems) in a triangular arrangement remained functional.

The documents summarize the applicable basic principles of antenna design and requirements that would govern the design of an antenna cluster for a specific proposed mission [the Jupiter Icy Moons Orbiter (JIMO)]. Candidate design concepts for realizing the aforementioned and other advantages for JIMO are analyzed.

*This work was done by Robert Clauss, Richard Lovick, Narayan Mysoor, and John Zitzelberger of Caltech for NASA's Jet Propulsion Laboratory. Further information is contained in a TSP (see page 1). NPO-40729*





National Aeronautics and  
Space Administration